Supporting Information

Transcriptome-wide Mapping of N^6-Methyladenosine via a Selective Chemical Labeling Method

Yalun Xie,[a,c] Shaoqing Han,[a,c] Qiming Li,[b] Zhentian Fang,[a] Wei Yang,[a] Qi Wei,[a] Yafen Wang,[a] Yu Zhou,[b] Xiaocheng Weng,[a] Xiang Zhou[a]*

[a] College of Chemistry and Molecular Sciences, Key Laboratory of Biomedical Polymers of Ministry of Education, Wuhan University, Wuhan, Hubei, 430072, P. R. China.

[b] College of Life Science, Wuhan University, Wuhan, Hubei, 430072, China.

[c] Contributed equally to this work.

* Corresponding Author, E-mail: xzhou@whu.edu.cn

List of contents

1. Materials

All chemicals were purchased from Sigama-Aldrich and Beijing Innochem unless mentioned otherwise. All of the unmodified, 5'-HEX, and 5'- phosphorylation oligonucleotides were synthesized and purified by GeneCreate Co., Ltd. (Wuhan, China). NO (99.9%) was supplied by Wuhan Newradar Special Gas Co., Ltd. The quantity of gas flow was exactly regulated by a mass flowmeter (HORIBA STEC, D519 MG, 0-10 sccm).

High-resolution mass spectra (HRMS) were recorded on Thermo Fisher Scientific LTQ Orbitrap Elite. ^{1}H nuclear magnetic resonance (NMR) and ^{13}C NMR, spectra were recorded on Bruker Avance 400 spectrometers. ESI-MS was collected on Thermo Fisher Scientific (Exactive). MALDI-TOF Mass Spectra were collected on Bruker autoflex max MALDI systems. HPLC data were recorded on an Agilent 1220 Infinity II LC System (Agilent Technologies), which was equipped with a SinoChrom ODS-BP C18 column (5 μm, 250 × 4.6 mm, Elite, Dalian, China). RNA concentration was quantified by NanoDrop 2000c (Thermo Scientific) or Invitrogen Qubit 4 (Thermo Scientific). Gel images were collected by the Pharos FX Molecular imager (Bio-Rad). qPCR assays were performed on CFX-96 RealTime System (Bio-Rad). The source of enzymes and other reagents used in this study were detailed in the corresponding procedure.

2. The sequences used in this study

Table S1. RNA oligos used in this work.

| Name	Sequence (5' to 3')
12nt-m^{6}A	UUUUUUm^{6}AUUUUU
12nt-Nm^{6}A	UUUUUUNm^{6}AUUUUU
12nt-Am^{6}A	UUUUUUAm^{6}AUUUUU
12nt-Bm^{6}A	UUUUUUBm^{6}AUUUUU
15nt-A	GACUCAAUAGCCGUA
15nt-m^{6}A	GACUCAAUm^{6}AGCCGUA
ODN-A	UGAUUCGAUGAUUCU
ODN-m^{6}A	UGm^{6}AUUCGAUGAUUCU
ODN-m^{6,6}A	UGm^{6,6}AUUCGAUGAUUCU
ODN-Bm^{6}A	UGBm^{6}AUUCGAUGAUUCU
ODN-Tm^{6}A	UGTm^{6}AUUCGAUGAUUCU
10nt-RT	5'-HEX/AGAATCATCG
12nt-RT	5'-HEX/AGAATCATCGAA
13nt-RT	5'-HEX/AGAATCATCGAAT
14nt-RT	5'-HEX/AGAATCATCGAATC
15nt-RT	5'-HEX/AGAATCATCGAATCA
FP-Library-qPCR	CAGACGTGTGCTCTTCCGATCT
RP-Library-qPCR	ACACGACGCTCTTCCGATCT

Table S2. Model RNA used in this work.

Name	Sequence (5' to 3')
MALAT1-2577-A	AGUAAUUACCAACUUAAUGUUUUUGCAUUGGACUUUGAGUUAAGAUUAUUUUUUAAAUCC
MALAT1-2577-m^{6}A	AGUAAUUACCAACUUAAUGUUUUUGCAUUGGm^{6}ACUUUGAGUUAAGAUUAUUUUUUAAAUCC

Table S3. Primers used for SELECT.

Name	Sequence (5' to 3')
*ZNF704*_80628578_up	tagccagtaccgtagtgcgtgGTAGAAGTCAAAATGGTCTTTTGAAAG
*ZNF704*_80628578_down	5'-phos/CCAGTGTTCTGGCTCTGTTTGTcagaggctgagtcgctgcat
*CDCA8*_37708389_up	tagccagtaccgtagtgcgtgCCCAGAAGTGCCCATTAAAAG
*CDCA8*_37708389_down	5'-phos/CCATCCTGTCAACTTTGGTGTCcagaggctgagtcgctgcat
*CAMSAP2*_200848137_up	tagccagtaccgtagtgcgtgTTAGATACATGACTGTTGTTCAGAGTAAG
*CAMSAP2*_200848137_down	5'-phos/CCTTCATTACTAATAGAACGAGTGATTCcagaggctgagtcgctgcat
*ZNF460*_57291319_up	tagccagtaccgtagtgcgtgCGACCCGCGATTGAAGG
*ZNF460*_57291319_down	5'-phos/CCTTCCACATTCACTGCACACAcagaggctgagtcgctgcat
*MAIP1*_199963837_up	tagccagtaccgtagtgcgtgTTAGTTTTTCACAGCAACTGCTAAAG
*MAIP1*_199963837_down	5'-phos/CCATAAGCTGATTTTTCCAAGAAAcagaggctgagtcgctgcat
*SLC35A5*_112580748_up	tagccagtaccgtagtgcgtgGTAGAAGTCAAAATGGTCTTTTGAAAG
*SLC35A5*_112580748_down	5'-phos/CCAGTGTTCTGGCTCTGTTTGTcagaggctgagtcgctgcat
*MALAT1*_2577_up	tagccagtaccgtagtgcgtgGGATTTAAAAAATAATCTTAACTCAAAG
*MALAT1*_2577_down	5'-phos/CCAATGCAAAAACATTAAGTcagaggctgagtcgctgcat
*MALAT1*_2614_up	tagccagtaccgtagtgcgtgGTCAGCTGTCAATTAATGC
*MALAT1*_2614_down	5'-phos/AGTCCTCAGGATTTAAAAAATAATCTTAACcagaggctgagtcgctgcat
qPCRF_SELECT	ATGCAGCGACTCAGCCTCTG
qPCRR_SELECT	TAGCCAGTACCGTAGTGCGTG

3. Chemical synthesis and NMR spectra

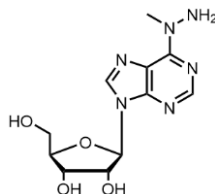**Synthesis of N[6]-nitroso-N[6]-methyladenosine (Nm[6]A).**
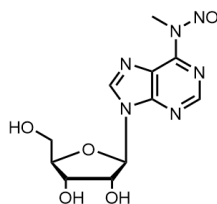
N[6]-methyladenosine (141 mg, 0.5 mmol) was dissolved in 50% aqueous CH_3CN (5.0 mL), NO gas was bubbling into the solution for 10 min in a chemical hood. After the completion of the reaction monitored by TLC, the solvent was evaporated in vacuo. The crude product was purified by silica gel chromatography (CH_2Cl_2/MeOH = 20 : 1) to give a yellowish powder (121 mg, 78 %).

^{1}H NMR (400 MHz, DMSO-D_6) δ (ppm): 8.95 (s, 1H), 8.90 (s, 1H), 6.12 (d, J = 5.4 Hz, 1H), 4.63 (t, J = 5.2 Hz, 1H), 4.23 – 4.19 (m, 1H), 4.01 (q, J = 3.9 Hz, 1H), 3.72 (dd, J = 12.0, 4.0 Hz, 1H), 3.64 – 3.57 (m, 4H). **^{13}C NMR** (101 MHz, DMSO-D_6) δ (ppm): 153.7, 151.9, 151.6, 145.7, 124.2, 88.2, 86.1, 74.4, 70.6, 61.6, 29.6.

HRMS (ESI+): calculated for $C_{11}H_{15}N_6O_5^+$ [M+H]$^+$: 311.1098, found: 311.1099.

**Synthesis of N[6]-amino-N[6]-methyladenosine (Am[6]A).**

N[6]-nitroso-N[6]-methyladenosine (78 mg, 0.25 mmol) and thiourea dioxide (81 mg, 0.75 mmol) was dissolved in MeOH (1.5 mL). Then 1.0 M NaOH solution (1.5 mL) was added. The mixture was stirred at 50 °C for 3 h. After evaporating in vacuo, the crude was purified by silica gel chromatography (CH_2Cl_2/MeOH = 15 : 1) to give a white powder (41 mg, 56%).

^{1}H NMR (400 MHz, DMSO-D_6) δ (ppm): 8.38 (s, 1H), 8.20 (s, 1H), 5.91 (d, J = 6.0 Hz, 1H), 5.57 (s, 2H), 5.45 (d, J = 6.2 Hz, 1H), 5.37 (dd, J = 7.0, 4.6 Hz, 1H), 5.19 (d, J = 4.8 Hz, 1H), 4.58 (dd, J = 11.1, 6.0 Hz, 1H), 4.14 (td, J = 4.8, 3.2 Hz, 1H), 3.96 (q, J = 3.5 Hz, 1H), 3.67 (ddd, J = 12.1, 4.6, 3.7 Hz, 1H), 3.55 (m, 4H). **^{13}C NMR** (101 MHz, DMSO-D_6) δ (ppm):153.9, 152.3, 145.0, 139.1, 119.1, 88.3, 86.3, 74.0, 71.0, 62.0.

HRMS (ESI+): calculated for $C_{11}H_{17}N_6O_4^+$ [M+H]$^+$: 297.1306, found: 297.1290.

Hydrazone formation of N[6]-amino-N[6]-methyladenosine with 2-pyridinecarboxaldehyde.
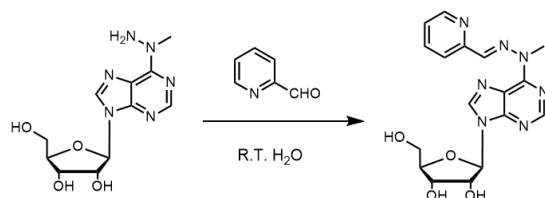

N[6]-amino-N[6]-methyladenosine (20 mg, 0.068 mmol) and 2-pyridinecarboxaldehyde (8.3 μL, 0.088 mmol) was dissolved in water (1.0 mL). The mixture was stirred at room temperature and the reaction monitored by TLC could be completed within 2 hours. After evaporating in vacuo, the crude was purified by silica gel chromatography (CH_2Cl_2/MeOH = 15 : 1, 0.2% Et$_3$N) to give a white solid (28 mg, 85%, complexed with one molecule of Et$_3$N).

¹H NMR (400 MHz, DMSO-D₆) δ (ppm): 8.74 (s, 1H), 8.65 (d, J = 4.3 Hz, 1H), 8.61 – 8.52 (m, 2H), 8.08 (s, 1H), 7.96 (td, J = 7.7, 1.7 Hz, 1H), 7.42 (dd, J = 7.4, 4.8 Hz, 1H), 6.09 (d, J = 5.6 Hz, 1H), 5.58 (d, J = 6.0 Hz, 1H), 5.28 – 5.21 (m, 2H), 4.64 (dd, J = 11.0, 5.6 Hz, 1H), 4.25 (dd, J = 8.9, 4.5 Hz, 1H), 4.04 (dd, J = 7.4, 3.7 Hz, 1H), 3.89 (s, 3H), 3.76 (dt, J = 12.1, 4.4 Hz, 1H), 3.65 (ddd, J = 12.1, 6.2, 3.9 Hz, 1H), 3.11 (q, J = 7.3 Hz, 6H), 1.25 (t, J = 7.3 Hz, 9H). **¹³C NMR** (101 MHz, DMSO-D₆) δ (ppm): 155.2, 153.7, 152.5, 151.6, 149.6, 142.2, 139.6, 137.0, 123.8, 121.7, 120.7, 88.0, 86.1, 74.4, 70.9, 61.8, 45.8, 30.8, 8.9.

HRMS (ESI+): calculated for $C_{17}H_{20}N_7O_4^+$ [M+H]⁺: 386.1571, found: 386.1552.

Synthesis of probe BA.

Probe **BA**, 26%
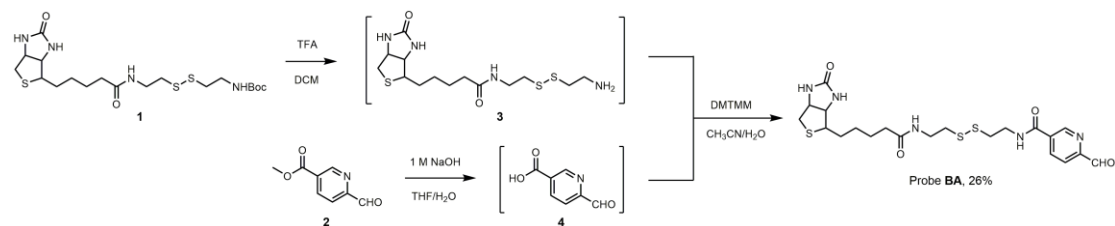
Compound **1** was synthesized referring to our previous report.[5] **1** (100mg, 0.209 mmol) was dissolved in 1.0 mL DCM and 300 μL trifluoroacetic acid (TFA) was added dropwise under stirring, the reaction mixture was stirred at room temperature for 1 h. After evaporating in vacuo and removal of the redundant TFA, the crude (**3**, trifluoroacetate) was directly used for the next step. Methyl 6-formylnicotinate (**2**, 41 mg, 0.25 mmol) was dissolved in 50% aqueous THF (4.0 mL), then 1.0 M NaOH solution (2.5 mL, 0.25 mmol) was added. The solution mixture was stirred at room temperature for 1 h under Ar atmosphere. After completion of the reaction, THF was evaporated in vacuo, the aqueous layer was acidified with 1.0 M HCl (3.0 mL) and extracted with EtOAc (3 × 10 mL), dried over Na₂SO4 and concentrated in vacuo to give a white solid (crude, **4**).[6] **3**, **4** and DMTMM (88 mg, 0.30 mmol) were dissolved in 50% aqueous CH₃CN (10 mL), then Et₃N (41 μL, 0.30 mmol) was added. The solution was stirred at 40 °C for 18 h. The reaction mixture was purified on silica gel chromatography followed by RP-HPLC (5% → 100% B in 35 min; A: H₂O; B: CH₃CN), gave a white powder (probe **BA**, 28 mg, 26%) after lyophilization.

¹H NMR (400 MHz, DMSO-D₆) δ (ppm): 10.05 (s, 1H), 9.20 (d, J = 1.4 Hz, 1H), 9.13 (t, J = 5.4 Hz, 1H), 8.42 (dd, J = 8.0, 1.7 Hz, 1H), 8.06 – 8.03 (m, 2H), 6.47 (s, 1H), 6.40 (s, 1H), 4.31 (dd, J = 7.8, 5.0 Hz, 1H), 4.18 – 4.09 (m, 1H), 3.61 (dd, J = 12.6, 6.3 Hz, 2H), 3.37 – 3.32 (m, 2H), 3.10 (ddd, J = 8.4, 6.1, 4.3 Hz, 1H), 2.95 (t, J = 6.8 Hz, 2H), 2.85 – 2.79 (m, 3H), 2.58 (d, J = 12.4 Hz, 1H), 2.08 (t, J = 7.3 Hz, 2H), 1.64 – 1.28 (m, 6H). **¹³C NMR** (101 MHz, DMSO-D₆) δ (ppm): 193.6, 172.7, 164.6, 163.2, 154.1, 149.4, 137.0, 133.6, 121.9, 61.5, 59.7, 55.9, 40.3, 39.3, 38.3, 37.8, 37.3, 28.6, 28.5, 25.7.

HRMS (ESI+): calculated for $C_{21}H_{30}N_5O_4S_3^+$ [M+H]⁺: 512.1454, found: 512.1458.

Hydrazone formation of N^6-amino-N^6-methyladenosine with BA to yield Bm^6A.
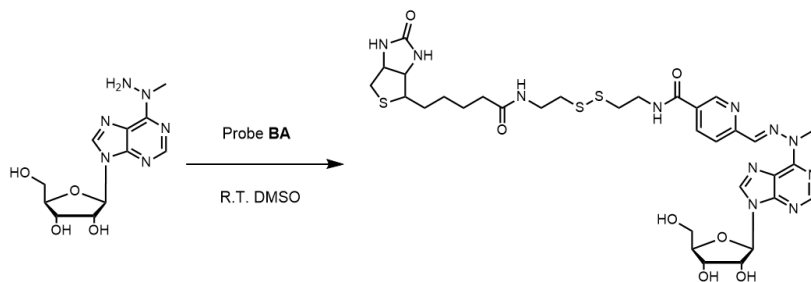

N^6-amino-N^6-methyladenosine (9.0 mg, 0.029 mmol) and **BA** (15 mg, 0.029 mmol) were dissolved in DMSO (1.0 mL). The mixture was stirred at room temperature for 12 h. After dryness in vacuo, the crude was purified by RP-HPLC (5% → 100% B in 35 min; A: H_2O; B: CH_3CN), gave a white powder (16 mg, 68%) after lyophilization.

^{1}H NMR (400 MHz, DMSO-D_6) δ (ppm): 9.02 (d, J = 1.6 Hz, 1H), 8.89 (t, J = 5.5 Hz, 1H), 8.70 (s, 1H), 8.58 (d, J = 8.3 Hz, 1H), 8.55 (s, 1H), 8.27 (dd, J = 8.3, 2.1 Hz, 1H), 8.07 (s, 1H), 8.00 (t, J = 5.6 Hz, 1H), 6.41 (s, 1H), 6.35 (s, 1H), 6.04 (d, J = 5.6 Hz, 1H), 5.51 (d, J = 6.0 Hz, 1H), 5.26 – 5.17 (m, 2H), 4.59 (dd, J = 10.9, 5.6 Hz, 1H), 4.29 (dd, J = 7.7, 5.0 Hz, 1H), 4.20 (td, J = 4.9, 3.6 Hz, 1H), 4.12 (ddd, J = 7.8, 4.5, 1.9 Hz, 1H), 3.99 (q, J = 3.6 Hz, 1H), 3.85 (s, 3H), 3.71 (dt, J = 11.9, 4.4 Hz, 1H), 3.65 – 3.55 (m, 3H), 3.37 – 3.35 (m, 2H), 3.08 (ddd, J = 8.5, 6.2, 4.3 Hz, 1H), 2.94 (t, J = 6.8 Hz, 2H), 2.85 – 2.77 (m, 3H), 2.57 (d, J = 12.4 Hz, 1H), 2.07 (t, J = 7.4 Hz, 2H), 1.62 – 1.27 (m, 6H). **^{13}C NMR** (101 MHz, DMSO-D_6) δ (ppm): 172.7, 165.2, 163.2, 157.4, 153.6, 152.5, 151.6, 148.6, 142.4, 138.6, 135.8, 129.1, 121.9, 120.1, 88.0, 86.1, 74.3, 70.8, 61.8, 61.5, 59.6, 55.9, 40.3, 39.3, 38.3, 37.8, 37.4, 35.6, 30.9, 28.6, 28.5, 25.7.
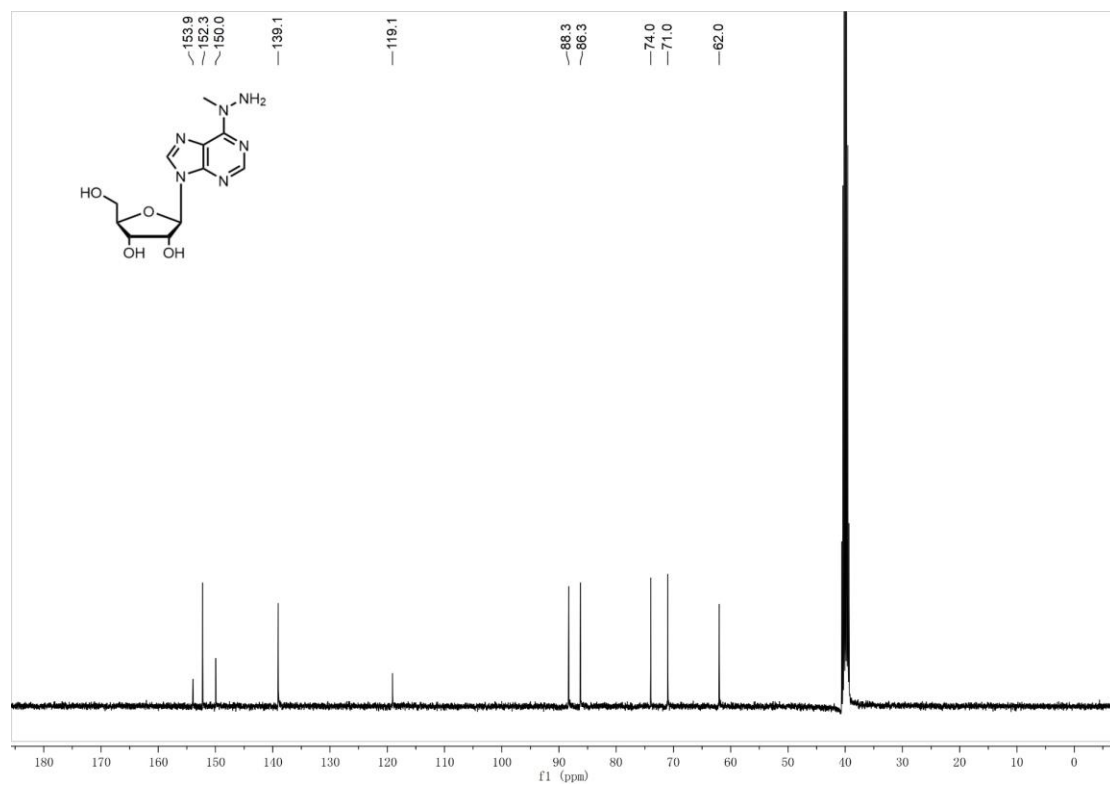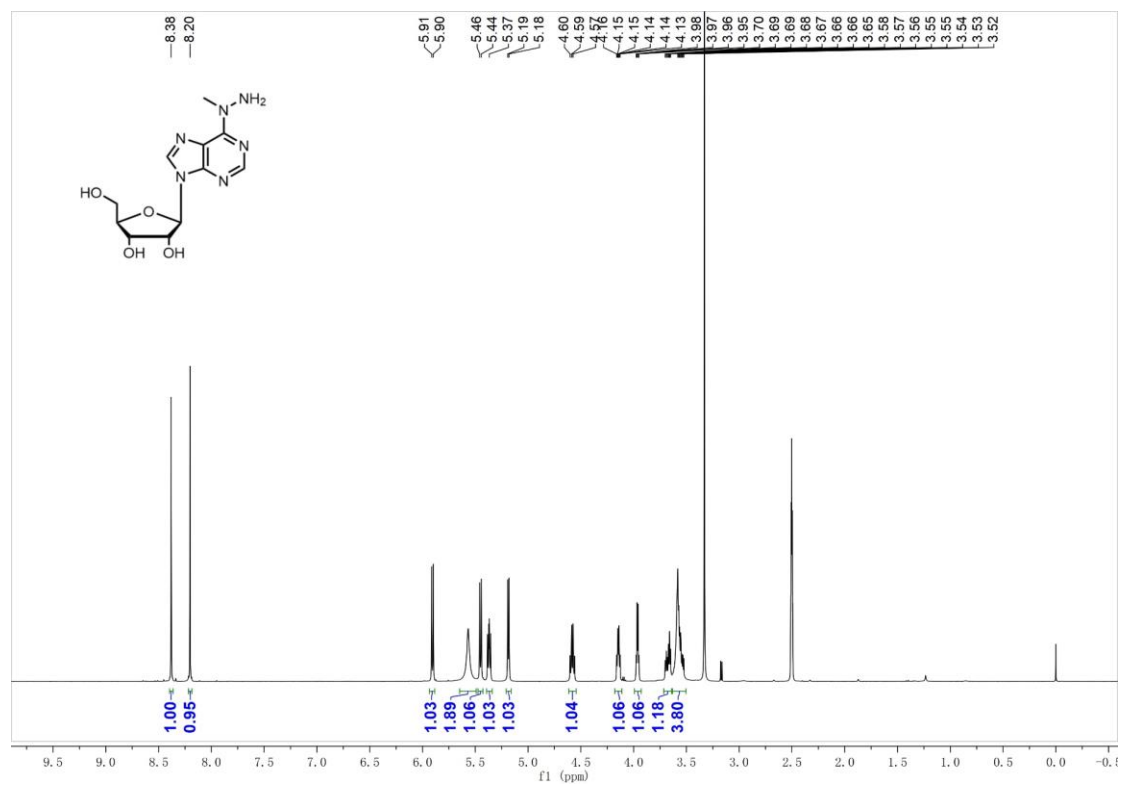
HRMS (ESI+): calculated for $C_{32}H_{44}N_{11}O_7S_3^+$ [M+H]$^+$: 790.2582, found: 790.2591.

¹H NMR, ¹³C NMR and HRMS characterization of synthesized chemical compounds.

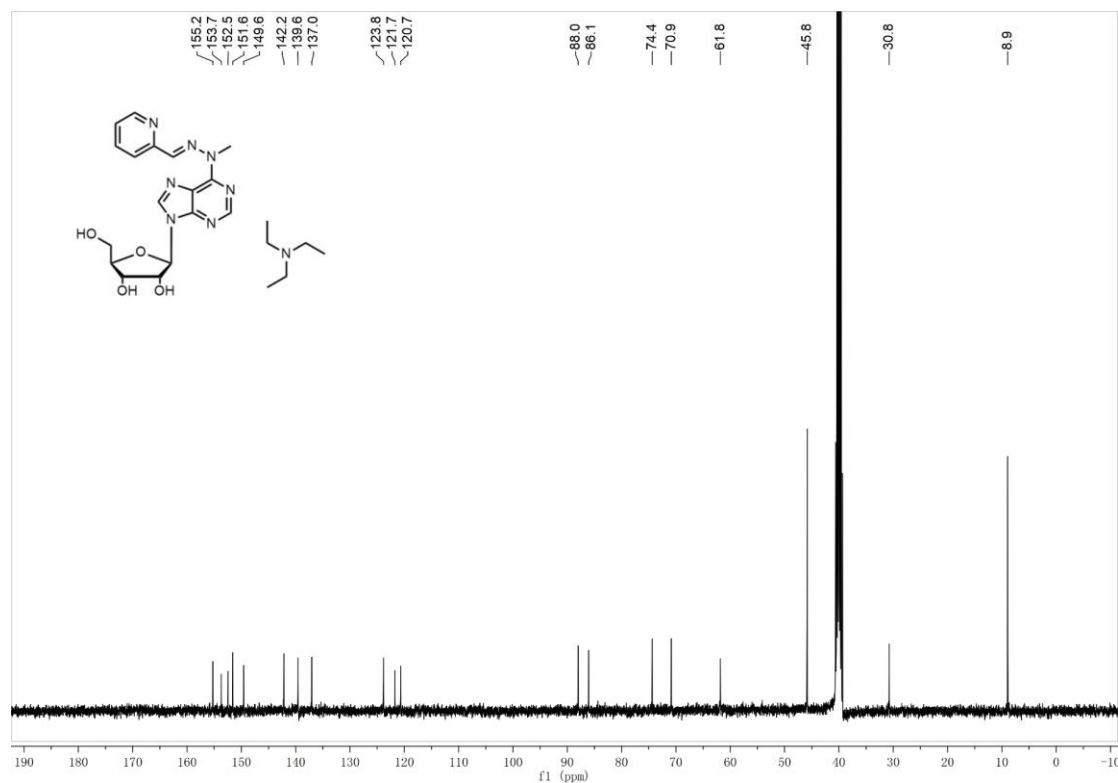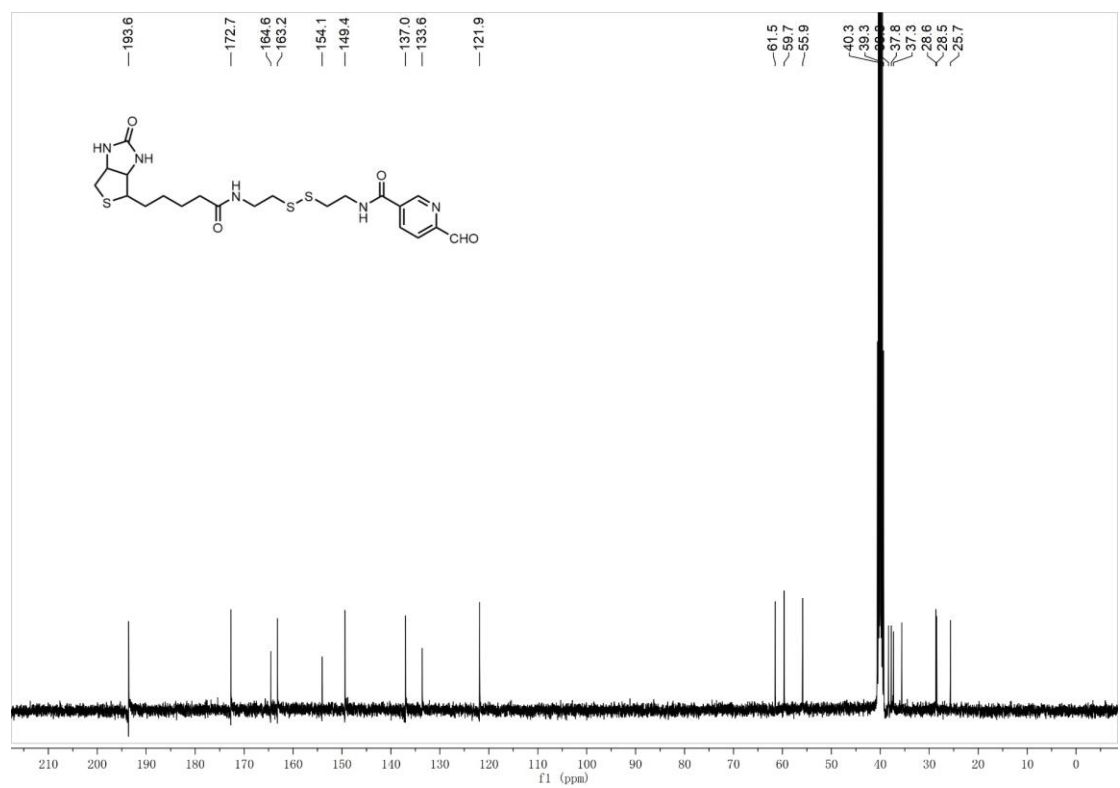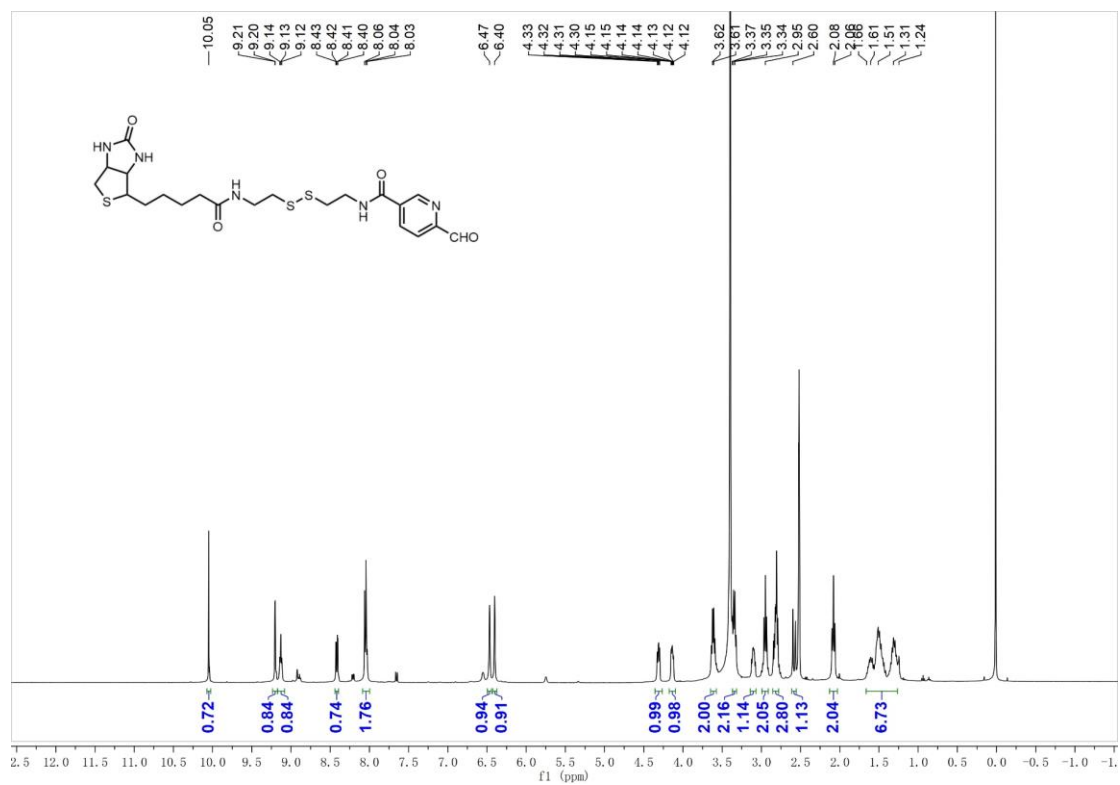¹H NMR and ¹³C NMR spectra of N⁶-nitroso-N⁶-methyladenosine. (solvent: DMSO-D₆)
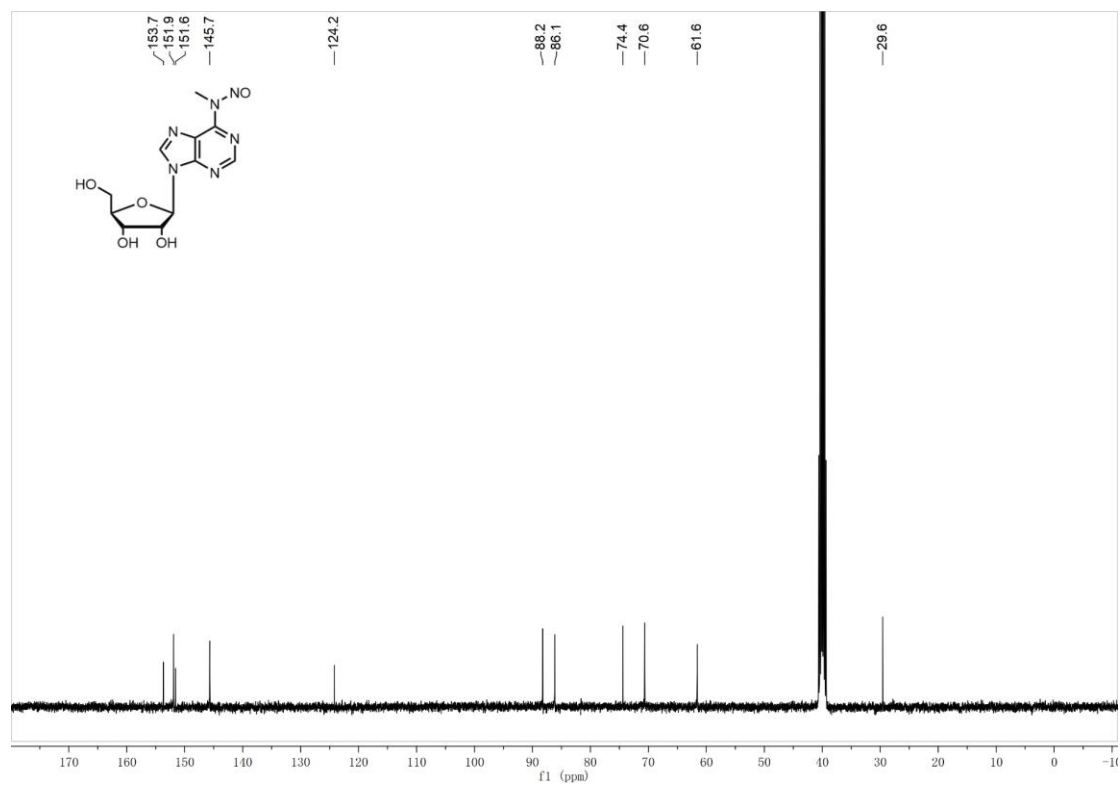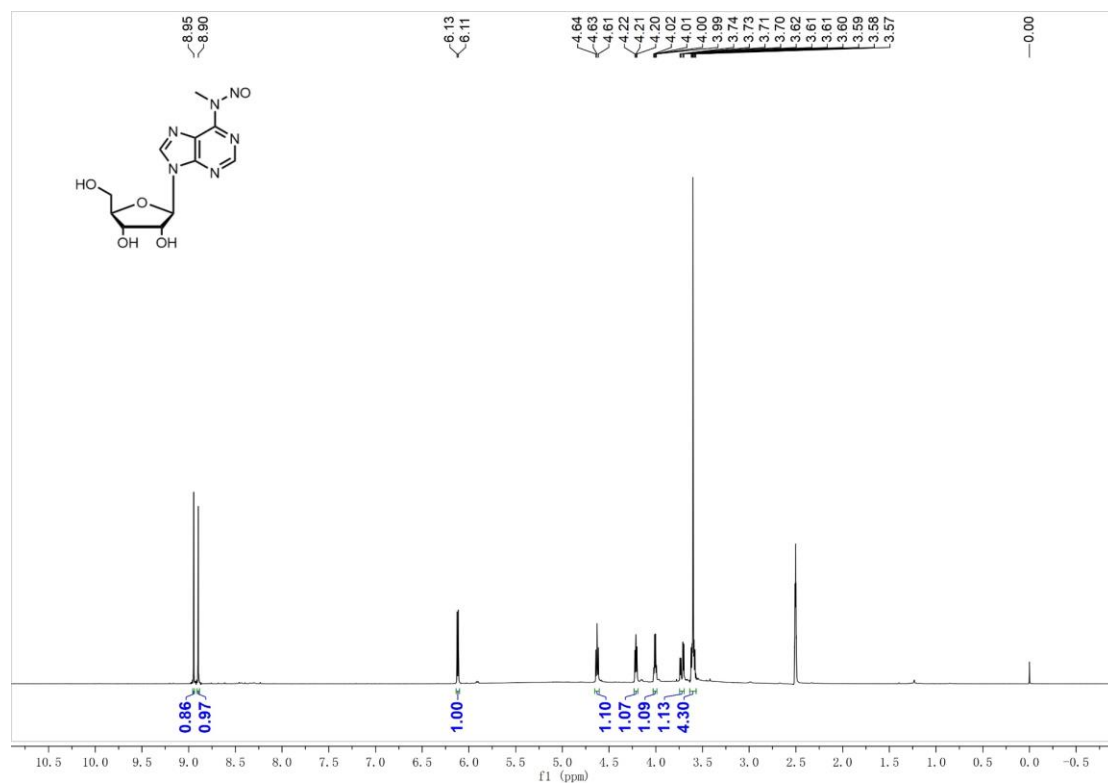
^{1}H NMR and ^{13}C NMR spectra of N^6-amino-N^6-methyladenosine. (solvent: DMSO-D$_6$)

^{1}H NMR and ^{13}C NMR spectra of the hydrazone synthesized by N^6-amino-N^6-methyladenosine with 2-pyridinecarboxaldehyde. (solvent: DMSO-D$_6$)
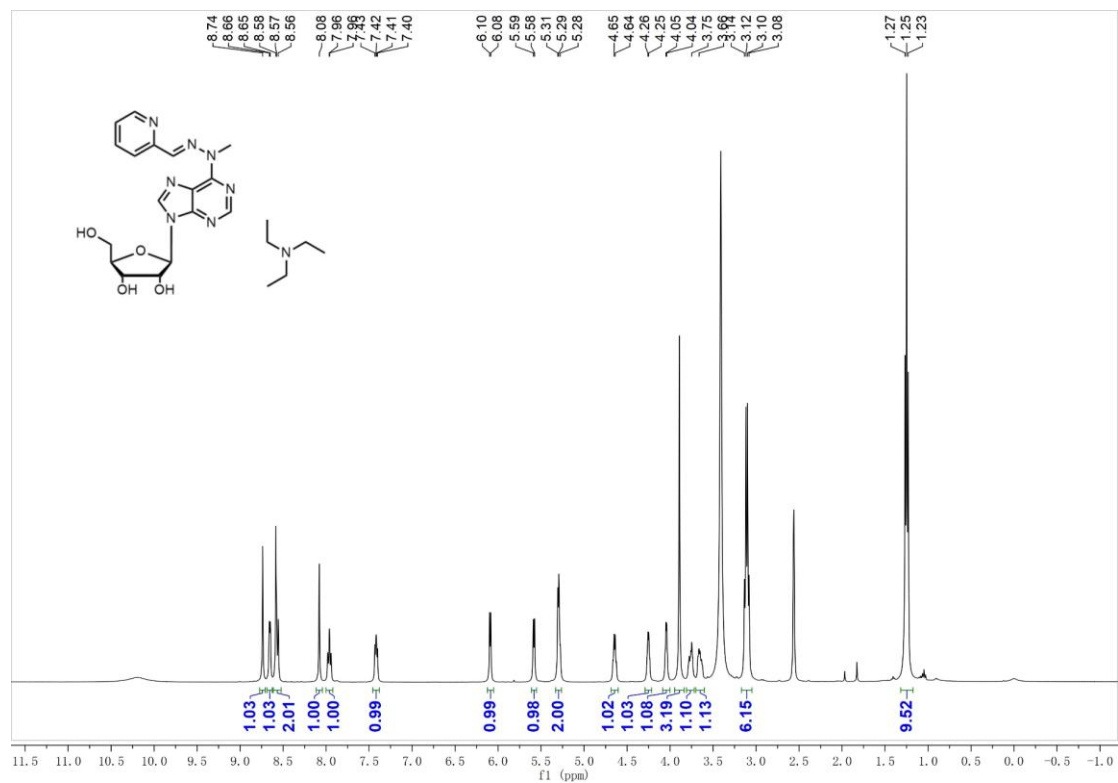
¹H NMR and ¹³C NMR spectra of probe **BA**. (solvent: DMSO-D₆)

¹H NMR and ¹³C NMR spectra of the hydrazone synthesized by N⁶-amino-N⁶-methyladenosine with **BA**. (solvent: DMSO-D₆)

The page displays a ¹H NMR spectrum (top) and a ¹³C NMR spectrum (bottom), each accompanied by the chemical structure of the biotin-disulfide-pyridine hydrazone adenosine conjugate.
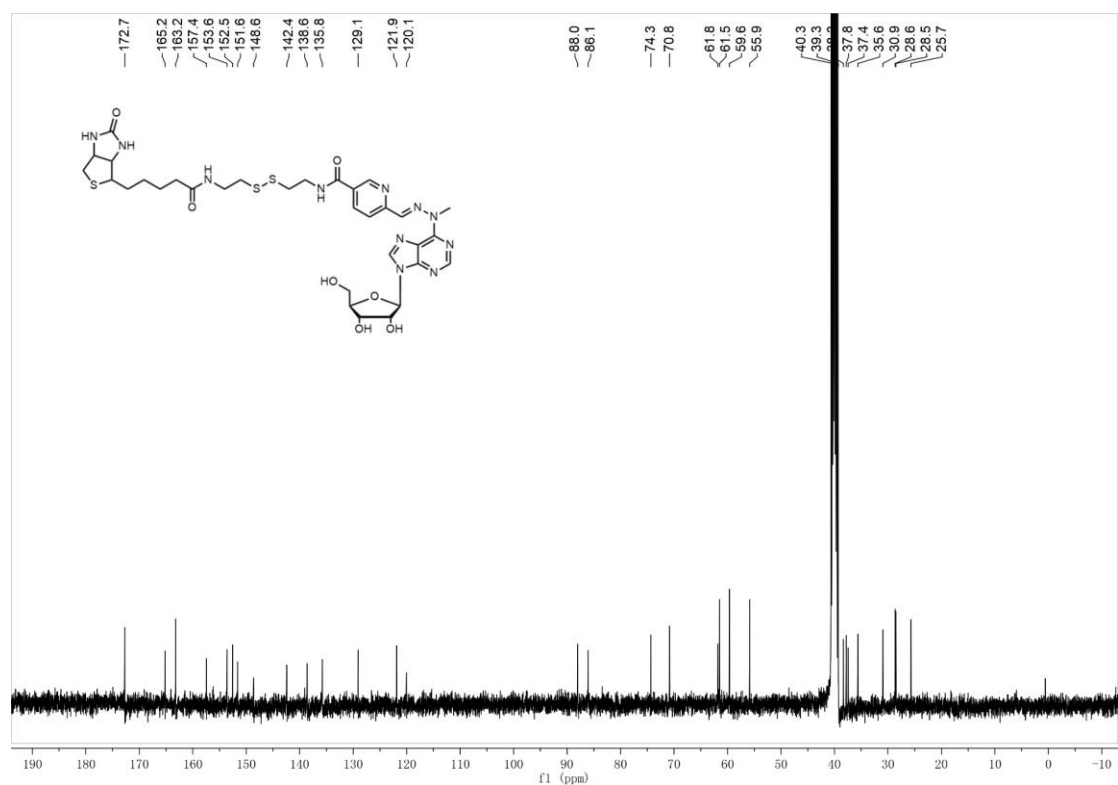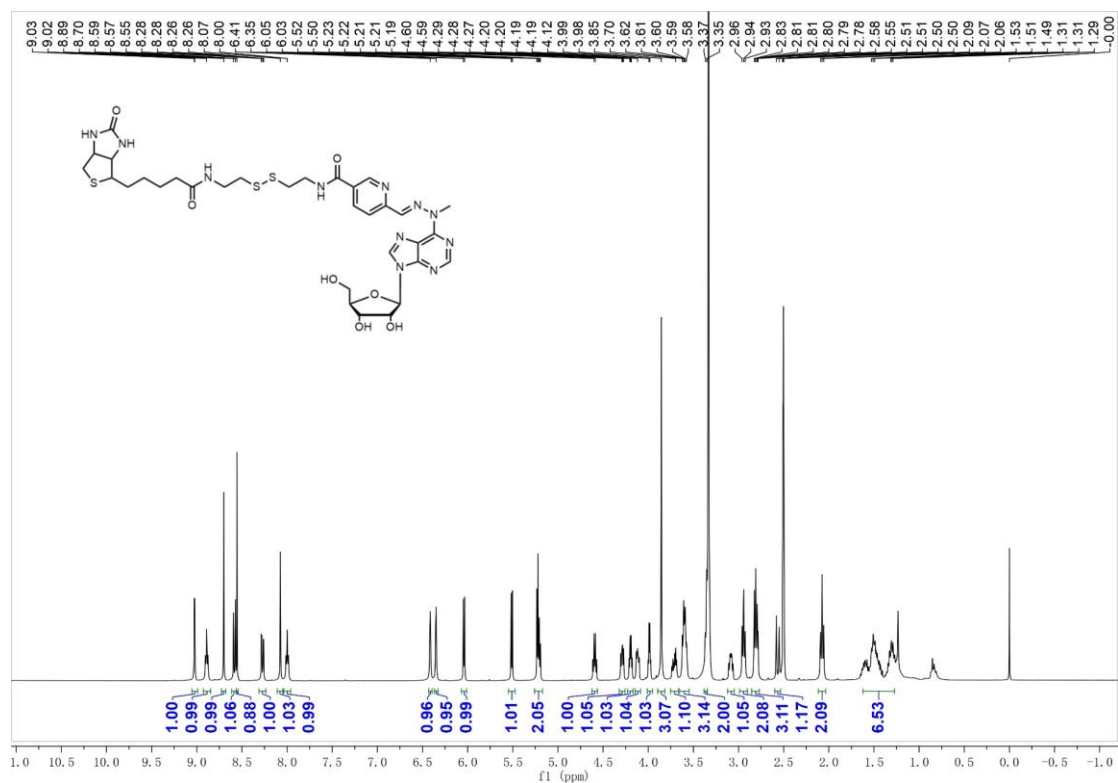
HRMS characterization of the hydrazone synthesized by N^6-amino-N^6-methyladenosine with **BA**.
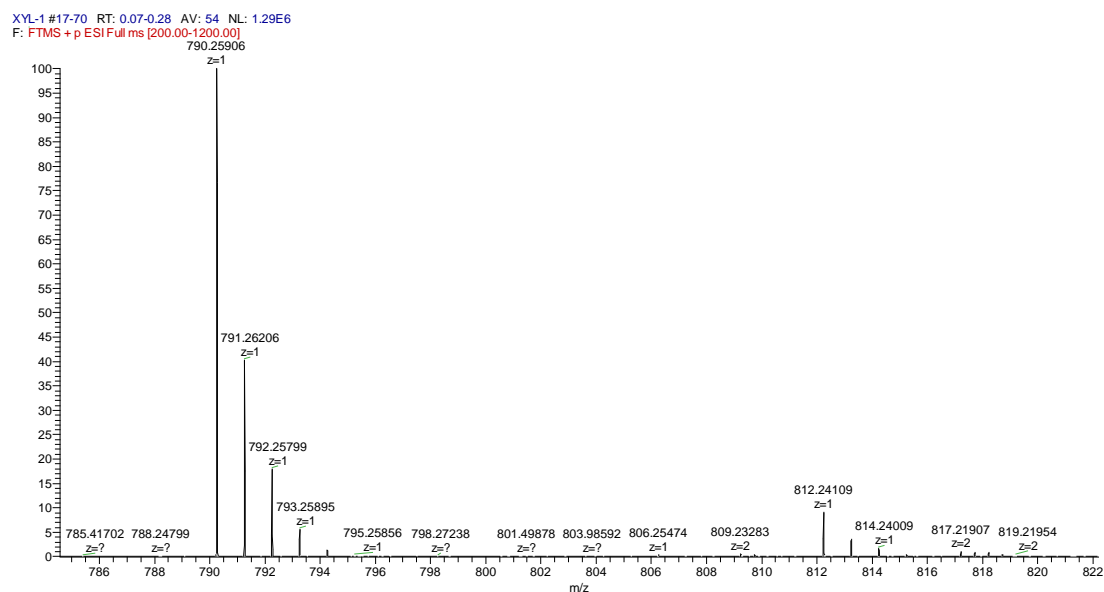
HRMS (ESI+): calculated for $C_{32}H_{44}N_{11}O_7S_3^+$ $[M+H]^+$: 790.2582, found: 790.2591.

4. HPLC analysis of Nm^{6}A to Am^{6}A and the proposed mechanism via TDO reduction
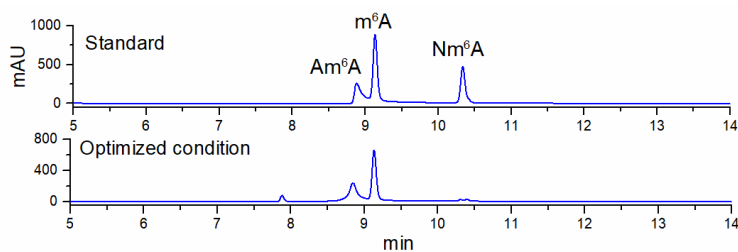
Fig. S1. HPLC chromatograms of Nm^{6}A to Am^{6}A. Optimized condition: 100 μM Nm^{6}A, 100 mM TDO, 300 mM Na$_2$CO$_3$/NaHCO$_3$, pH 10.0, 50 °C, 1000 rpm, 5 min.. Conversion rate caculated by HPLC at 260 nm using external standards: 60%. HPLC gradient: A: 50 mM ammonium acetate; B: CH$_3$CN; 35 °C, 1.0 mL/min, 260 nm, 0-20 min, 5-100% B.

Fig. S2. The proposed mechanism for TDO reduction of Nm⁶A to Am⁶A.[7] Thiourea dioxide (TDO) is known to yield sulfoxylic acid under base and heat treatment,[8] which is a potent reducing reagent.

5. HPLC analysis and mass spectra of 12nt-m⁶A, 12nt-Nm⁶A, 12nt-Am⁶A, 12nt-Bm⁶A

Fig. S3. MALDI-TOF-MS spectra of 12nt-m⁶A. $[M+H^+]_{cal}=3648.4$, $[M+H^+]_{obs}=3650.5$.

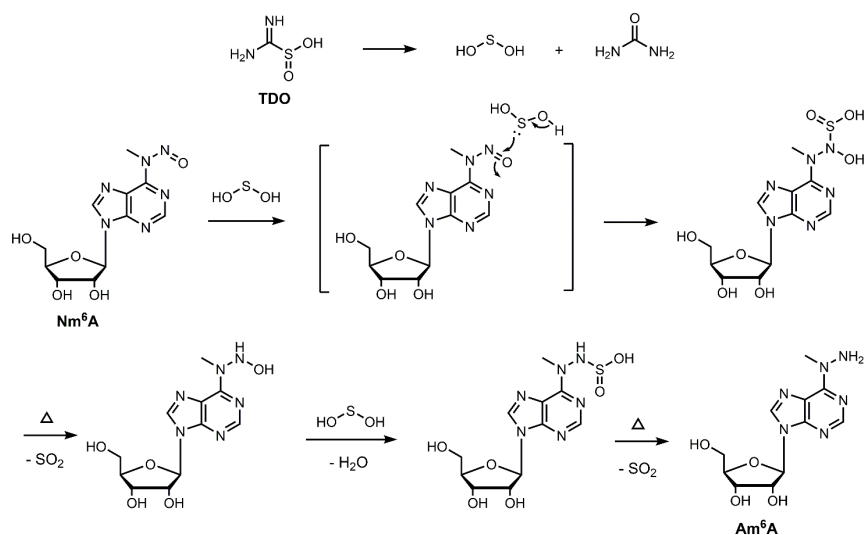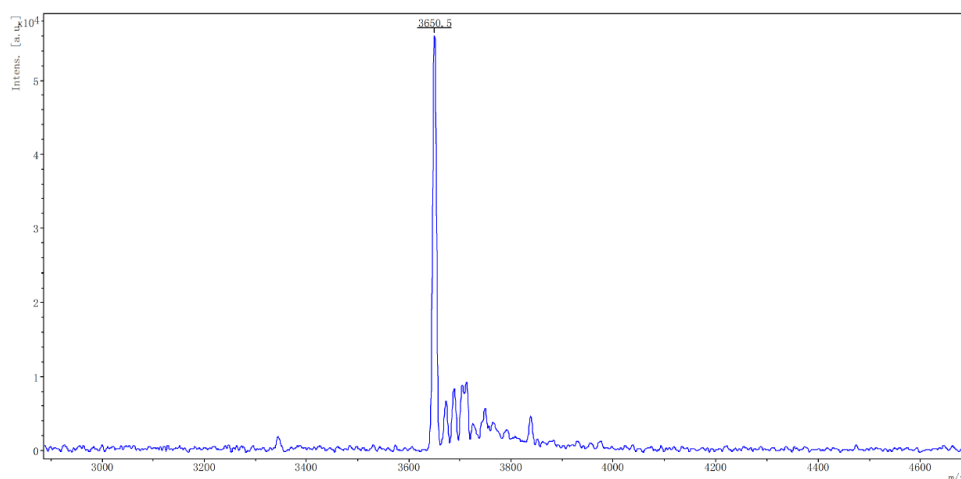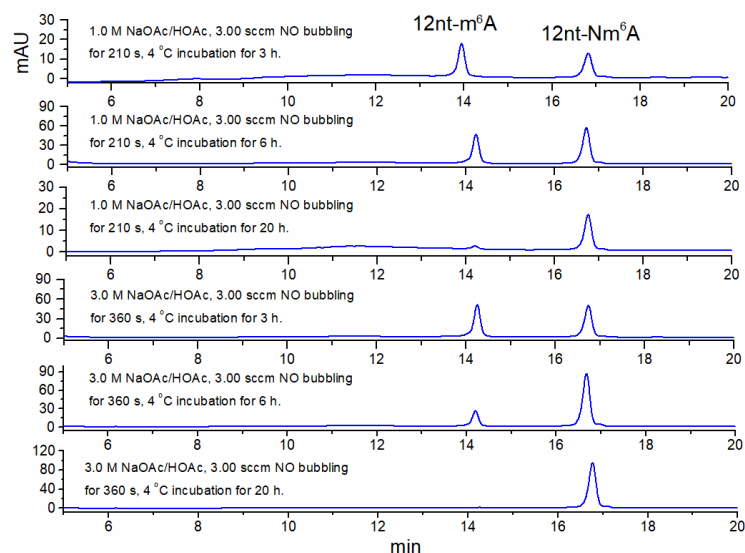Fig. S4. HPLC chromatograms of 12nt-m6A (0.2 nmol) to 12nt-Nm6A via N-nitrosation. We observed that a longer NO bubbling time yield a higher concentration of NO in solution, which accelerated the reaction process. After incubation, RNA oligo was purified using ethanol precipitation and submitted to HPLC analysis. HPLC gradient: A: 50 mM TEAA (pH 7.5); B: CH_3CN; 35 °C, 1.0 mL/min, 260 nm, 0-5-25 min, 5-10-15% B. Conversion rate calculated by HPLC at 260 nm: >95%.

Fig. S5. LTQ XL ESI-MS spectra of 12nt-Nm6A. [M-H-]$_{cal}$ =3675.4, [M-H-]$_{obs}$ =3678.5.
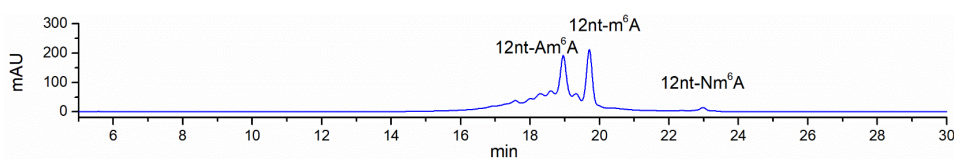
Fig. S6. HPLC chromatograms of 12nt-Nm6A to 12nt-Am6A via TDO reduction. Optimized condition: 1.0 nmol 12nt-Nm6A, 100 mM TDO, 300 mM Na_2CO_3/$NaHCO_3$, 2 mM EDTA, pH 10.0, 50 °C, 1000 rpm, 10 min, total volume 50 μL. After incubation, the solution was directly submitted to HPLC analysis. HPLC gradient: A: 50 mM

TEAA (pH 7.5); B: CH₃CN; 35 °C, 1.0 mL/min, 260 nm, 0-5-25 min, 5-8-13% B. Conversion rate calculated by HPLC at 260 nm: 46%.
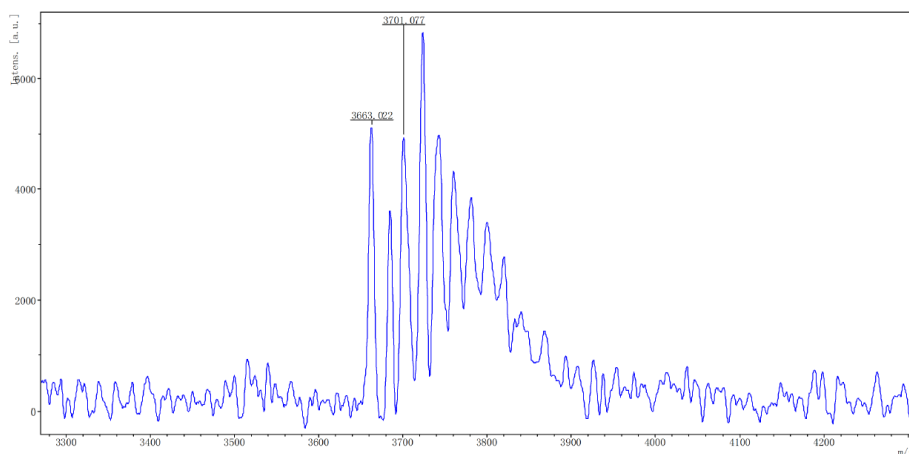
Fig. S7. MALDI-TOF-MS spectra of 12nt-Am^{6}A. [M+H$^+$]$_{cal}$ =3663.4, [M+H$^+$]$_{obs}$ =3663.0.
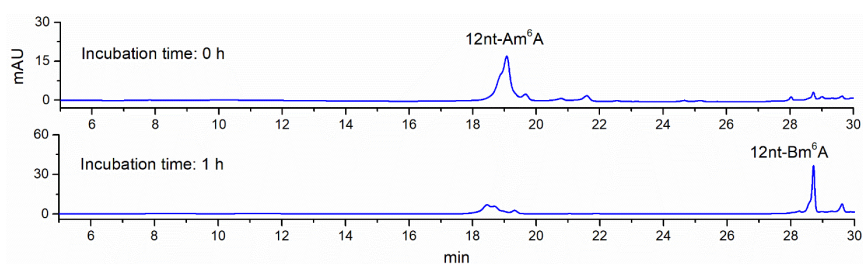
Fig. S8. HPLC chromatograms of 12nt-Am^{6}A to 12nt-Bm^{6}A via **BA** labeling. Optimized condition: 0.2 nmol 12nt-Am^{6}A, 2.0 mM **BA**, 100 mM MES, 10% DMF, pH 5.5, 37 °C, 1000 rpm, 1.0 h, total volume 50 µL. After incubation, the solution was purified using ethanol precipitation and submitted to HPLC analysis. HPLC gradient: A: 50 mM TEAA (pH 7.5); B: CH₃CN; 35 °C, 1.0 mL/min, 260 nm, 0-5-21-36 min, 5-8-12-100% B. Conversion rate calculated by HPLC at 260 nm: >90%.
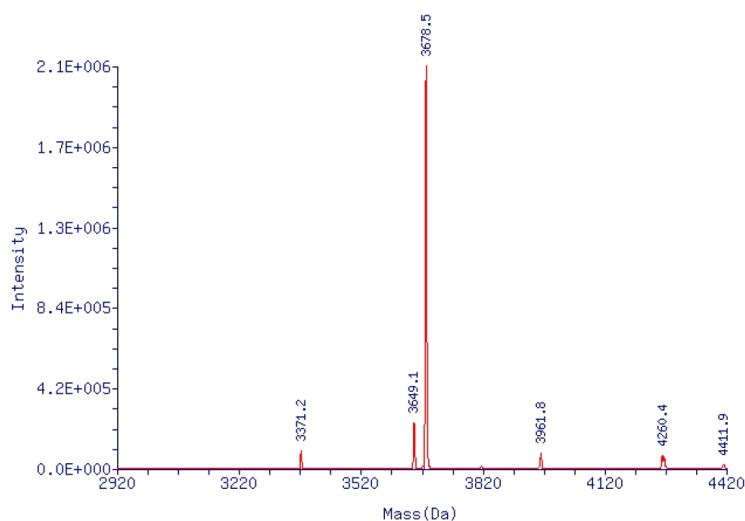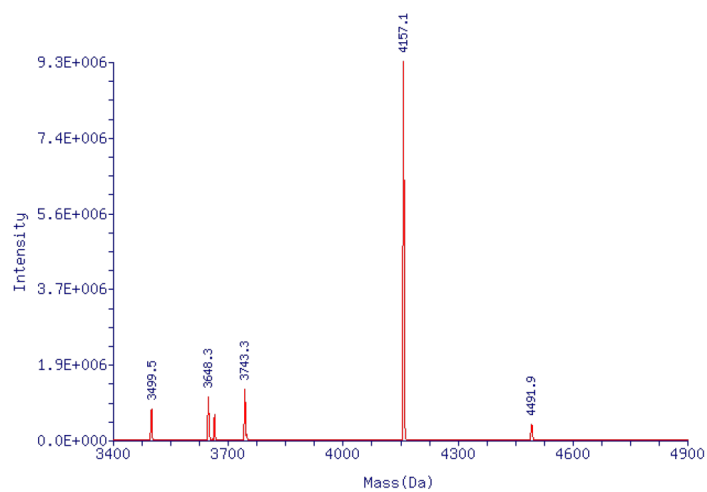

Fig. S9. LTQ XL ESI-MS spectra of 12nt-Bm^{6}A. [M-H$^-$]$_{cal}$ =4154.5, [M-H$^-$]$_{obs}$ =4157.1.

6. Three-step chemical treated 15nt-m^{6}A was enzymatically digested into ribonucleosides and subjected to LC-HRMS analysis

Chemical treated 15nt-m^{6}A was digested according to the enzymatic digestion procedure. LC-HRMS confirmed the chemical labeling of m^{6}A at each step.

a. N-nitrosation
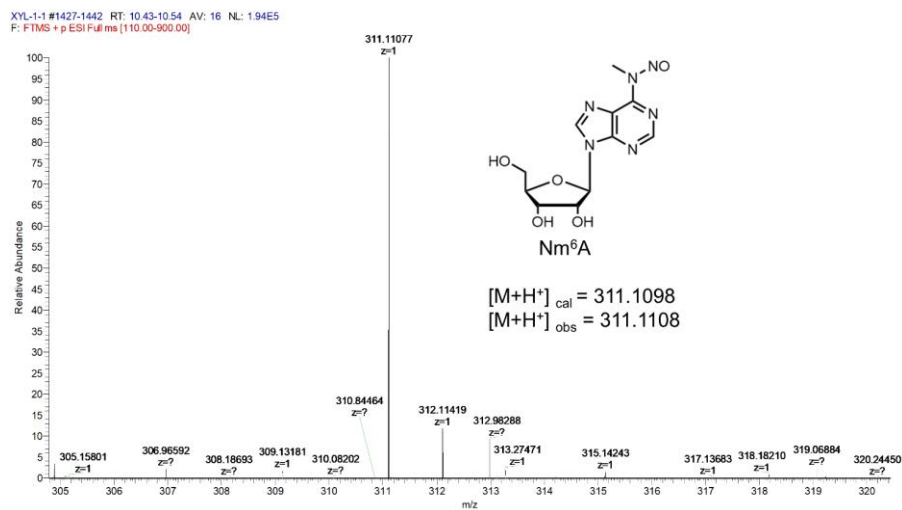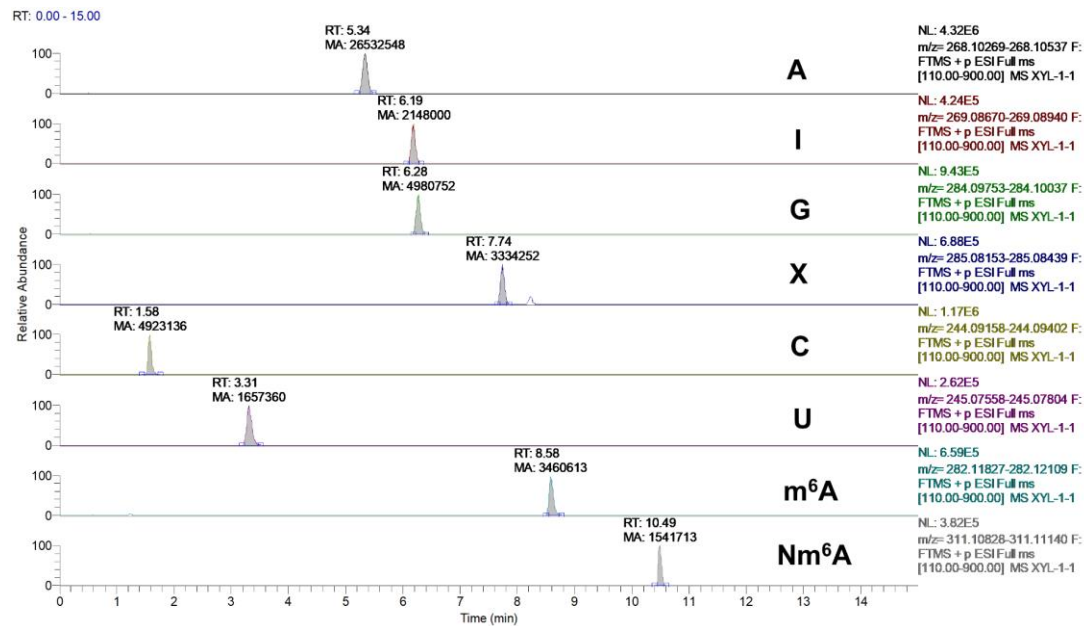
Fig. S10. LC-HRMS analysis of digested ribonucleosides for N-nitrosation. I, $[M+H^+]_{cal}$= 269.0881, $[M+H^+]_{obs}$ = 269.0888; X, $[M+H^+]_{cal}$= 269.0881, $[M+H^+]_{obs}$ = 269.0888. Nm^{6}A, $[M+H^+]_{cal}$ = 311.1098, $[M+H^+]_{obs}$ = 311.1108.

b. TDO reduction
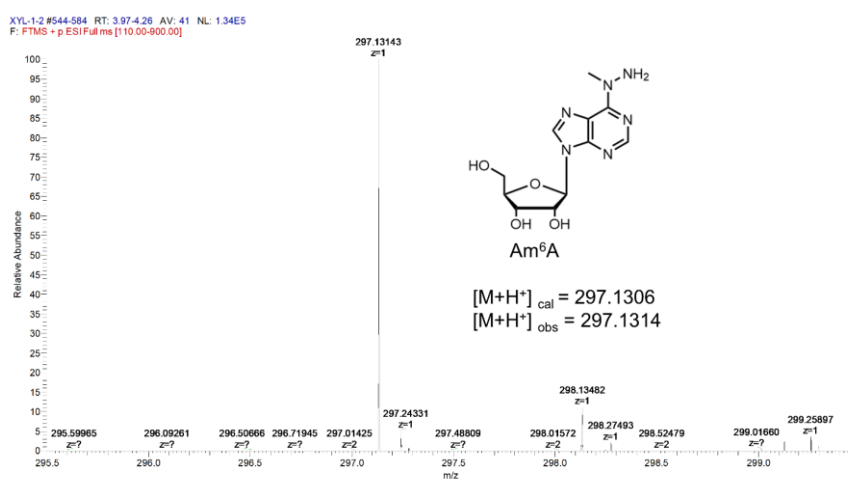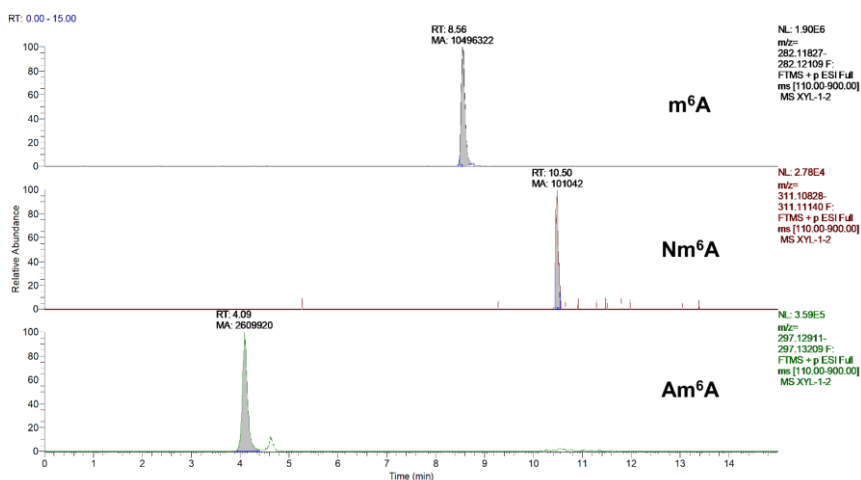
Fig. S11. LC-HRMS analysis of digested ribonucleosides for TDO reduction. Am^{6}A, [M+H$^+$]$_{cal}$= 297.1306, [M+H$^+$]$_{obs}$ = 297.1314.

c. Biotinylation (Probe BA labeling)
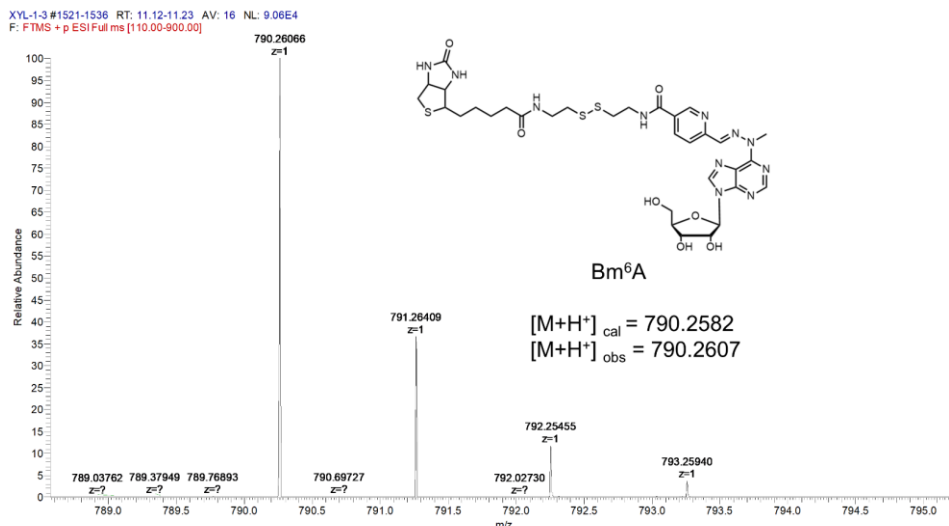
Fig. S12. LC-HRMS analysis of digested ribonucleosides for TDO reduction. Bm^6A, $[M+H^+]_{cal}$ = 790.2582, $[M+H^+]_{obs}$ = 790.2607. Compared to Fig. S11, the estimated conversion rate of Am^6A to Bm^6A is 90%.

7. Investigations on RNA degradation caused by NO/O_2 treatment

In an ice bath, 181 ng 60 nt RNA (Table S2, MALAT1-2577-A, quantified by Qubit 4) in 200 μL sodium acetate buffer (1.0 M or 3.0 M, pH 4.5) was bubbled with NO gas (3.00 sccm), after 4 °C incubation for 30 h, RNA was purified by ice ethanol precipitation and 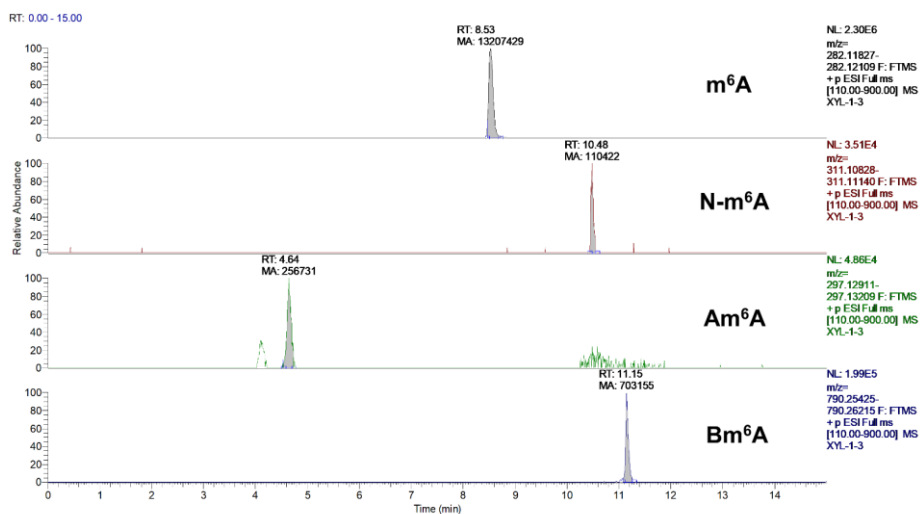quantified by Qubit 4 Fluorometer. Here shows the different times of NO bubbling and the buffer capacity affect the RNA degradation.

Condition	1.0 M no NO	1.0 M 1.0 min	1.0 M 2.0 min	1.0 M 3.0 min	1.0 M 3.5 min	1.0 M 4.0 min	3.0 M no NO	3.0 M 4.0 min	3.0 M 5.0 min	3.0 M 6.0 min	3.0 M 7.0 min	3.0 M 8.0 min
Recovery rate	81%	73%	63%	51%	42%	< 10%	60%	46%	43%	40%	38%	29%
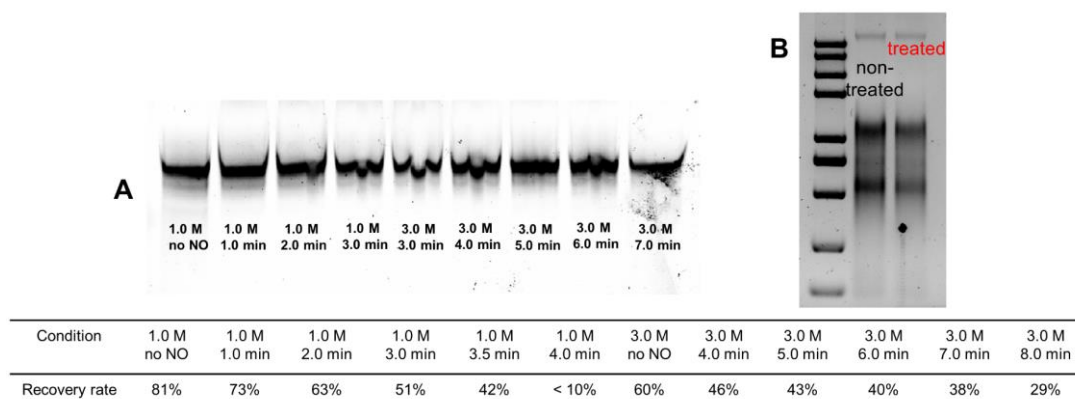
Fig. S13. (A) Denaturing PAGE analysis and RNA quantification of different NO bubbling time and buffer concentrations. These results confirmed that our N-nitrosation conditions do not cause large RNA degradation within the rational range of NO bubbling time. (B) Agarose gel electrophoresis analysis confirmed HEK-293T total RNA did not degrade under the condition of TDO reduction.

The subsequent experiment used HEK-293T total RNA to perform N-nitrosation under optimal condition for N-nitrosation (3.00 sccm NO, bubbling for 6.0 min, 3.0 M sodium acetate buffer, 2 mM EDTA, pH 4.5, incubation at 4 °C for 20 h), more than 60% of RNA was recovered using RCC purification and Qubit 4 quantification.

For m^6A-ORL-Seq, approximately 20% of biotinylated RNA was recovered through three-step labeling and purification (Qubit 4 quantification).

8. N-nitrosation treated HEK-293T total RNA was enzymatically digested into ribonucleosides and quantified using LC-MS/MS

5.0 μg HEK-293T total RNA (60-200 nt), 3.00 sccm NO, bubbling for 6.0 min, 3.0 M sodium acetate buffer, 2 mM EDTA, pH 4.5, incubation at 4 °C for 4-30 h. RNA was purified using RCC and enzymatically digested into ribonucleosides, following subjected to LC-MS/MS (Shimadzu, LCMS-8050, equipped with an Agilent ZORBAX Eclipse C18 column) analysis.
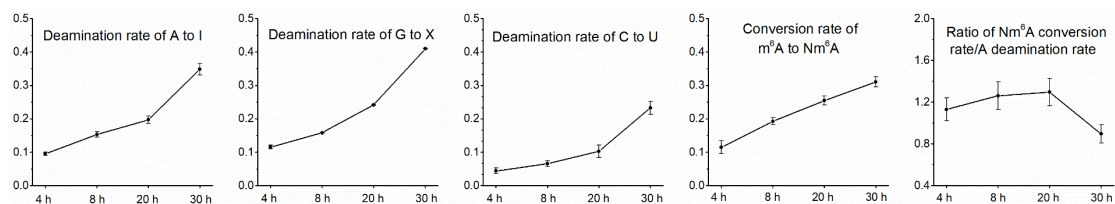
Fig. S14. LC-MS/MS analysis of chemical treated total RNA after enzymatic digestion. Quantitation was performed on the basis of peak areas of characteristic nucleoside-to-base ion mass transitions of 268.1-to-136.1 (A), 269.1-to-137.1 (I), 284.1-to-152.1 (G), 285.1-to-153.0 (X), 244.1-to112.1 (C), 245.1-to113.0 (U), 282.1-to-150.1 (m^{6}A) and 311.1-to-179.1 (Nm^{6}A). In consideration of reducing the mutation rates and increasing m^{6}A labeling efficiency, we chose 20 h as the optimal incubation time, since such the case has the highest ratio of Nm^{6}A/I and moderate labeling efficiency.

9. Dot blot assay
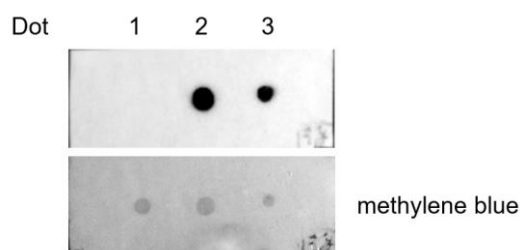
Fig. S15. Dot blot assay confirmed selective biotinylation of m^{6}A in MALAT1-2577-m^{6}A. Dot 1: three-step labeling products of MALAT1-2577-A; Dot 2: three-step labeling products of MALAT1-2577-m^{6}A; Dot 3: a mixture containing three-step labeling products of MALAT1-2577-A and 5'-biotinylated DNA.
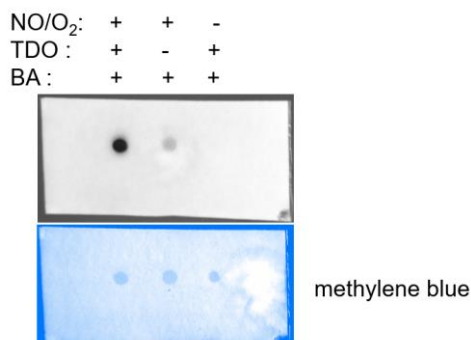
Fig. S16. Dot blot assay indicated evident biotinylation only in the case of three-step labeling of 293T total RNA.

10. Library construction

This protocol is a modified version according to a previous report.[9]

For each RNA sample, perform the following step for library constructions:

a. PNK treatment

Reagents	Volume (μL)
10× PNK buffer (NEB, B0201S)	1
T4 PNK (NEB, M020L)	1
RNase inhibitor (40 U/μL, Thermo, EO0382)	1
RNA sample	5
RNF H$_2$O	2
Total	10

Mix well and incubate at 37 ℃ for 1 h and then heat-inactivation of PNK at 65 ℃ for 20 min, conduct the next step directly.

b. 3' RNA linker ligation

Add 1 μL 10 μM 3' RNA linker (5'rAPP-AGATCGGAAGAGCGTCGTG-3SpC3) into 10 μL RNA sample, and mix well. Heat at 65°C for 5 min and then chill on ice immediately. Prepare the ligation mix as follow:

Reagents	Volume (μL)
10× RNA ligation buffer (NEB, B0216S)	2.5
100 mM DTT	2.5
50% PEG8000 (NEB, B1004S)	7.5
T4 RNA ligase2, truncated KQ (NEB, M0373L)	1
RNase inhibitor (40 U/μL, Thermo, EO0382)	1
Total	14.5

Add the ligation mix into the RNA mix and mix well.

Incubate at 25 ℃ for 2 h and 16 ℃ overnight.

Add 1 μL 5' Deadenylase (NEB, M0331S) into the ligation mix followed by incubating at 30 °C for 1 h and then add 1 μL RecJf (NEB, M0264) followed by incubating at 37 °C for another 1 h to remove excess 3' RNA linker. RNAs are purified by Oligo Clean & Concentrator (OCC, Zymo), and eluted in 12 μL RNF H$_2$O completely.

c. Reverse transcription

Add 1 μL 2 μM RT primer (5'-ACACGACGCTCTTCCGATCT-3') into 10 μL RNA sample, and mix well. Heat at 65 °C for 5 min and then chill on ice immediately. Prepare the reverse transcription mix as follow:

Reagents	Volume (μL)
5× First Strand Buffer (Invitrogen)	4
10 mM each dNTP mix (Thermo)	2
100 mM DTT	1
Superscript III (Invitrogen)	1
RNase inhibitor (40 U/μL, Thermo, EO0382)	1
Total	9

Add the reverse transcription mix into RNA and mix well.

Incubate at 25 ℃ for 3 min, 42 ℃ for 7 min, 52 ℃ for 30 min and hold at 4 ℃. Do not raise samples above 37 ℃ to avoid denaturing conditions.

Add 1 μL Exonuclease I (NEB, M0293S) and incubate at 37 °C for 30 min to digest excess RT primers.

Add 10 μL 1.0 M NaOH, 10 μL 0.5 M EDTA, 10 μL H_2O and incubate at 65 ℃ for 15 min to digest RNA templates. The cDNAs are purified by OCC, and eluted in 7 μL RNF H_2O completely.

d. 5' adaptor ligation

Add 0.3 μL 80 μM 5' adaptor (5Phos- NNNNNNNNNNAGATCGGAAGAGCACACGTCTG-3SpC3) and 1 μL DMSO into 6 μL cDNA sample, and mix well. Heat at 65 °C for 5 min and then chill on ice immediately. Prepare the ligation mix as follow:

Reagents	Volume (μL)
10 × RNA ligation buffer (NEB, B0216S)	2
0.1M ATP (NEB, N0437A)	0.2
50% PEG8000 (NEB, B1004S)	9
T4 RNA ligase 1, high concentration (NEB, M0437M)	1.5
Total	12.7

Add the ligation mix into cDNA and mix well.

Incubate at 25 ℃ overnight. The cDNAs are purified by OCC, and eluted in 30 μL RNF H_2O completely.

e. qPCR to test cycles

Prepare qPCR mix as follow:

Reagents	Volume (μL)
2 × Hieff PCR SYBR Green Master Mix (Yeasen)	5
Forward primer (10 μM)	1
Reverse primer (10 μM)	1
cDNA	3
Total	10

f. PCR amplification

Prepare PCR mix as follow:

Reagents	Volume (μL)
NEB Next Ultra II Q5 Master Mix (M0544L)	25
Universal primer (NEB)	1
Index primer (NEB)	1
cDNA	23
Total	50

Mix well and run the PCR amplification as follow:

Temperature	Time	Cycle
98 ℃	30 s	1
98 ℃	10 s	referring to

65 ℃	75 s	qPCR results
65 ℃	5 min	1
4 ℃	Hold	1

g. Cleanup of PCR Reaction

Allow the beads to warm to room temperature for at least 30 minutes before use. Add 45 μL (0.9×) VAHTS® DNA Clean Beads (Vazyme) to the PCR reaction. Mix well by pipetting up and down at least 10 times. Incubate samples on bench top for at least 5 minutes at room temperature. Place the tube on an appropriate magnetic stand to separate the beads from the supernatant. After 5 min (or when the solution is clear), carefully remove and discard the supernatant. Add 200 μL freshly prepared 80% ethanol to the tube while in the magnetic stand. Incubate at room temperature for 30 seconds, and then carefully remove and discard the supernatant for twice. Air dry the beads for up to 5 min while the tube is on the magnetic stand with the lid open. Remove the tube from the magnetic stand. Elute the DNA target from the beads by adding 23 μL of 0.1 × TE. Mix well by pipetting up and down at least 10 times. Incubate for 5 min at room temperature. Place the tube on the magnetic stand. After 5 min (or when the solution is clear), transfer 21 μL to a new tube for and store it at -20°C.

Libraries were sequenced on the Illumina HiSeq X-Ten platform with a paired-end model (PE150).

11. m^{6}A sites and m^{6}Am sites were identified in the m^{6}A-ORL-Uniq peaks that not overlapped with MeRIP

Based on N6-modified adenosine induced RT truncation, we found 559 high-confidence m^{6}A sites in the m^{6}A-ORL-Uniq peaks. Likewise, we performed the same screening to dig out m^{6}Am sites stopped at BCA motif. 990 m^{6}Am sites were obtained from the m^{6}A-ORL-Uniq peaks. Metagene profiling of 990 m^{6}Am sites revealed a significant enrichment at 5' UTR which was more remarkable than m^{6}Am peaks derived from m^{6}Am-Seq[10]. These results confirmed m^{6}A-ORL-Seq enables detect m^{6}A and m^{6}Am that MeRIP cannot provide.
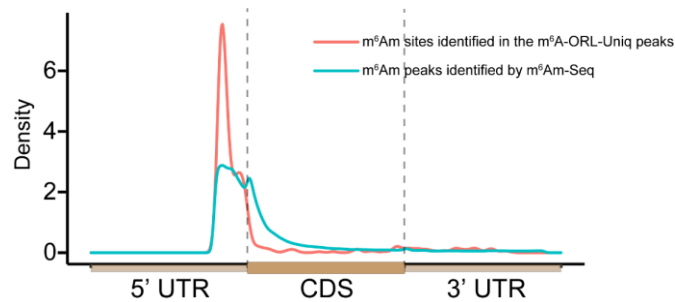

Fig. S17. Metagene profiling of m^{6}Am sites identified in the m^{6}A-ORL-Uniq peaks and m^{6}Am peaks identified by m^{6}Am-Seq.

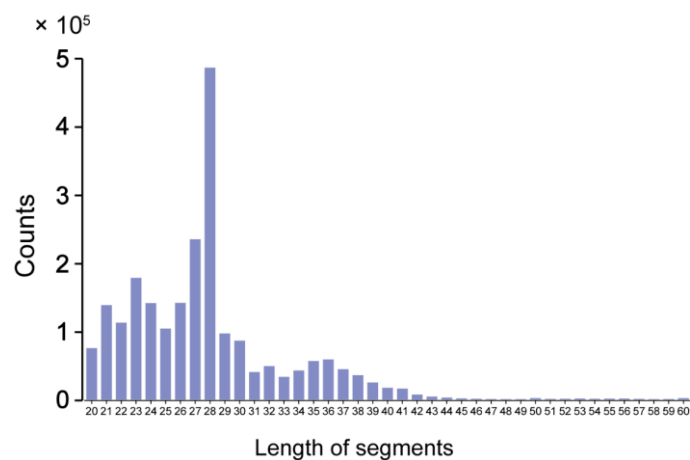## 12. Base-resolution analysis of m⁶A model RNA via m⁶A-ORL-Seq

Fig. S18. Statistics on counts of different lengths of segments in 60 nt model m⁶A-RNA revealed a specific RT-truncation at site 32 (m⁶A site).

13. Synthesis of several 15 nt RNA oligo (ODN-X) containing N6-modified adenosine via a post-synthetic method

Recently, we developed a post-synthetic method based on 6-iodopurine for the facile synthesis of modified RNA oligo.[11]
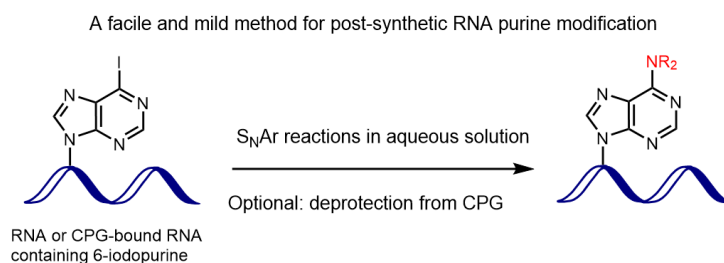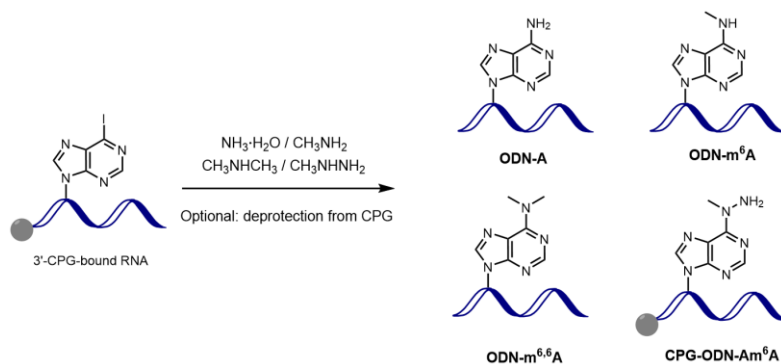

Fig. S19. Illustration of our unpublished post-synthetic method for synthesis of RNA oligo containing N6-modified adenosine.
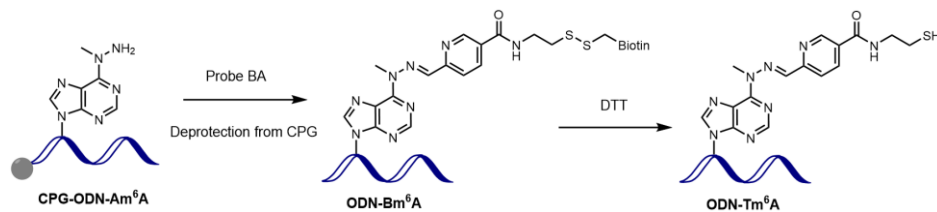
Fig. S20. The schematic diagram of synthesis of ODN-X.

a. Procedure for synthesis of ODN-A

2 nmol 3'-CPG bound 6-iodopurine (6IP) modified RNA oligo (5'-UG-6IP-UUCGAUGAUUCU-3'-CPG) was incubated in 28% aqueous ammonia (200 μL) at 65 °C for 40 min, then concentrated in vacuo and incubated with a mixture of DMSO and Et$_3$N·3HF (200 μL, 1:1) at 60 °C for 2.5 h. At last RNA oligonucleotides were purified using ethanol precipitation and following HPLC purification. HPLC yield: 40%.

b. Procedure for synthesis of ODN-m^{6}A

2 nmol 3'-CPG bound 6-iodopurine (6IP) modified RNA oligo (5'-UG-6IP-UUCGAUGAUUCU-3'-CPG) was incubated in 28% aqueous ammonia and 40% aqueous methylamine (200 μL, 1:1) at 65 °C for 40 min, then concentrated in vacuo and incubated with a mixture of DMSO and Et$_3$N·3HF (200 μL, 1:1) at 60 °C for 2.5 h. At last RNA oligonucleotides were purified using ethanol precipitation and following HPLC purification. HPLC yield: >95%.

c. Procedure for synthesis of ODN-m^{6,6}A

The mixture of 2 nmol 3'-CPG bound 6-iodopurine (6IP) modified RNA oligo (5'-UG-6IP-UUCGAUGAUUCU-3'-CPG), 200 mM dimethylamine and 200 mM Et$_3$N was incubated at 37 °C for 6 h. After centrifugation and removal of the supernatant, the CPG-bound RNA was incubated in 28% aqueous ammonia and 40% aqueous methylamine (200 μL, 1:1) at 65 °C for 40 min, then concentrated in vacuo and incubated with a mixture of DMSO and Et$_3$N·3HF (200 μL, 1:1) at 60 °C for 2.5 h. At last RNA oligonucleotides were purified using ethanol precipitation and following HPLC purification. HPLC yield: >95%.

d. Procedure for synthesis of ODN-Bm^{6}A

The mixture of 2 nmol 3'-CPG bound 6-iodopurine (6IP) modified RNA oligo (5'-UG-6IP-UUCGAUGAUUCU-3'-CPG), 100 mM methylhydrazine sulfate and 200 mM Et$_3$N was incubated at 30 °C for 14 h. After centrifugation and removal of the supernatant, the CPG-bound RNA was washed once with 50 RNF H$_2$O. After removal of the supernatant, The mixture of CPG-bound RNA, 5 mM BA, 100 mM MES (pH 5.5) and 10% DMF was incubated at 37 °C for 1 h. Then remove the supernatant, the residue was incubated in 28% aqueous ammonia and 40% aqueous methylamine (200 μL, 1:1) at 65 °C for 40 min, then concentrated in vacuo and incubated with a mixture of DMSO and Et$_3$N·3HF (200 μL, 1:1) at 60 °C for 2.5 h. At last RNA oligonucleotides were purified using ethanol precipitation and following HPLC purification. HPLC yield: 68%.

e. Procedure for synthesis of ODN-Tm^{6}A

ODN-Bm^{6}A was incubated with 100 μL of 100 mM DTT at 42 °C for 30 min. Then RNA oligonucleotides were purified using ethanol precipitation and following HPLC purification. HPLC yield: >95%.
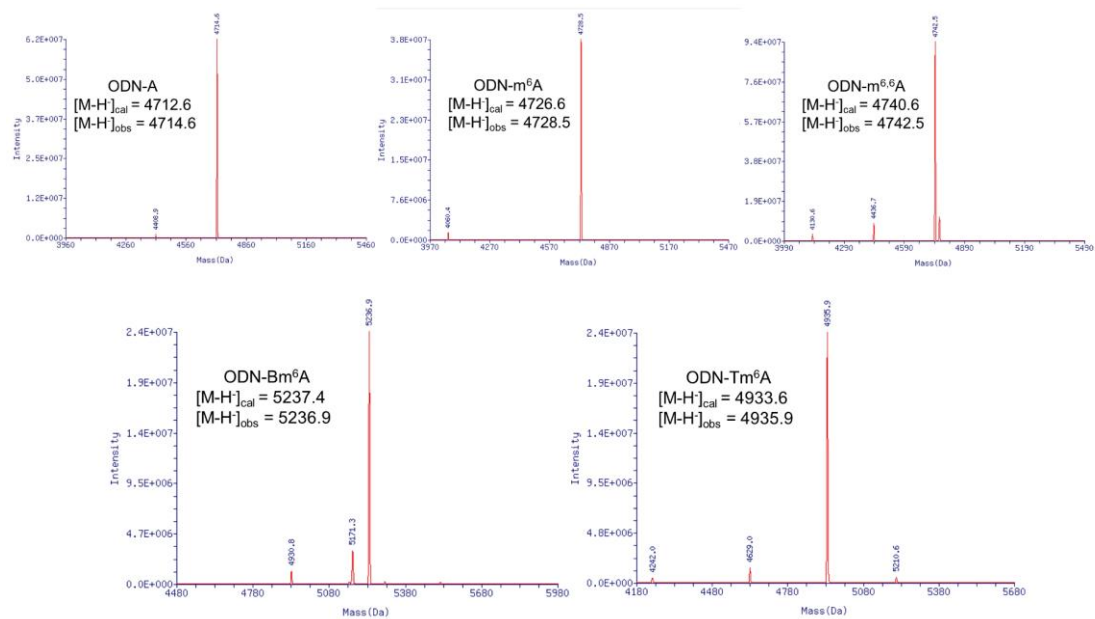
Fig. S21. LTQ XL ESI-MS characterization of synthetic ODN-X.

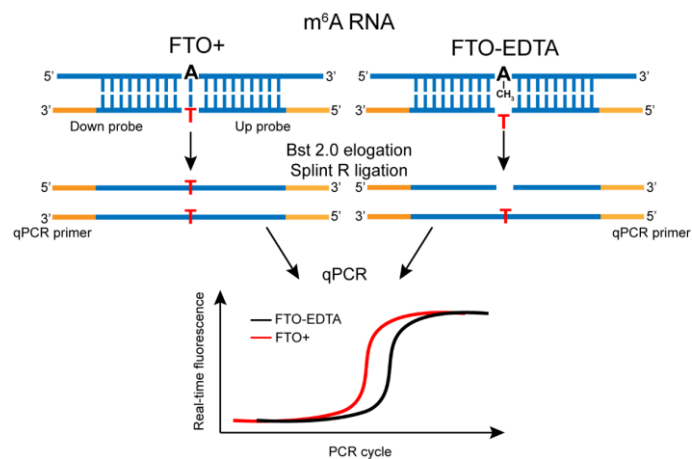## 14. SELECT validation of several m⁶A sites identified by m⁶A-ORL-Seq in HEK-293T

Fig. S22. Illustration of the SELECT (single-base elongation- and ligation-based qPCR amplification method) m⁶A detection method.[4]
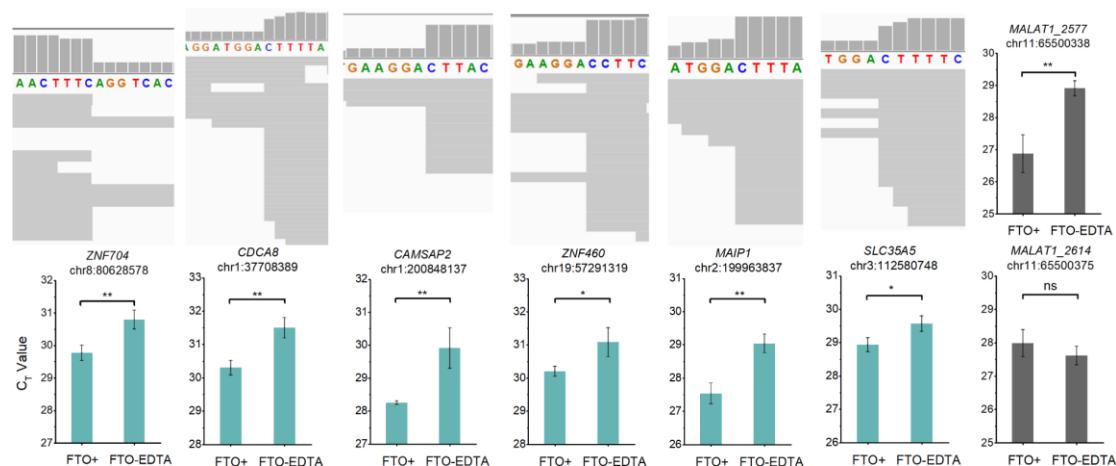
Fig. S23. SELECT validation of six individual sites detected by m⁶A-ORL-Seq in HEK-293T. These six sites were not detected by current reported methods. 2577m⁶A and 2614A in *MALAT1* were used as controls. n = 3 biological replicates × 3 technical replicates. *p<0.05; **p<0.01; ns, non-significant by t-test (two-tailed).

15. Discussions on m⁶A-ORL-Seq and recent reported sodium nitrite-based methods for m⁶A detection

Two chemical methods (nitrite sequencing[12] and NOseq[13]) based on sodium nitrite have been recently reported for m⁶A detection at single-base resolution. These two chemical-based methods are valuable, but not applicable to transcriptome-wide analysis of m⁶A. The well-designed threshold value (mutation rate of A to G) for m⁶A detection in several specific sequences is not all workable for practical RNA samples of great complexity. What's more, they are powerless for the location of m⁶A sites of low modification level unless the combination with m⁶A immunoprecipitation.

To be honest, after coming to an idea of selective N-nitrosation of m⁶A, we chose the most used sodium nitrite as well. During the investigation, we found very low mapped reads in high-throughput sequencing data when applying the sodium nitrite-based method to transcriptome-wide m⁶A analysis. Also, the condition of N-nitrosation using sodium nitrite is more severe than NO solution system. Here show the mutation rates in high-throughput sequencing data for 60 nt model RNA (*MALAT1*-2577-m⁶A) using different conditions. It turns out our N-nitrosation condition is more mild and suitable for transcriptome-wide sequencing.

Table S4. Mutation rates in high-throughput sequencing data for model RNA using different conditions.

Entry	Reaction Buffer	NaNO₂ conc.	Temp.	Reaction Time	A-to-G mutation rate	C-to-T mutation rate
1	-	-	-	-	0.1%	0.3%
2[a]	5% acetic acid	1.0 M	22 °C	5 h	48.0%	37.6%
3[b]	200 mM citrate buffer, pH 4.0	1.0 M	37 °C	6 h	18.0%	12.2%
4	m⁶A-ORL-Seq				6.8%	2.3%

[a] The optimal condition reported from nitrite sequencing.

[b] The NOseq-like condition developed by us. The mutation rate is consistent with the NOseq.

16. Basic information of sequencing data for HEK-293T cell line

Table S5. Basic information of sequencing data for HEK-293T cell line.

Sample	Average read length	Total input reads	Total mapped rate	Mismatch rate per base
MeRIP_rep1	176	24,641,629	94.60%	0.45%
MeRIP_rep2	181	18,034,642	94.45%	0.47%
MeRIP_input	146	23,553,991	94.64%	0.43%
m^6A-ORL_rep1	118	61,942,766	90.35%	2.41%
m^6A-ORL_rep1_input	169	71,727,812	95.05%	0.46%
m^6A-ORL_rep2	97	30,441,540	83.34%	3.17%
m^6A-ORL_rep2_input	92	30,572,879	82.50%	3.25%

17. Stoichiometry distribution of methylation levels of m^6A sites identified by different methods based on the dataset of MAZTER-Seq

Technically, MAZTER-Seq provided the normalized cleavage efficiencies of m^6A sites, which is a relative (not absolute) quantification. Here, the normalized cleavage efficiencies were simplified into A fraction.
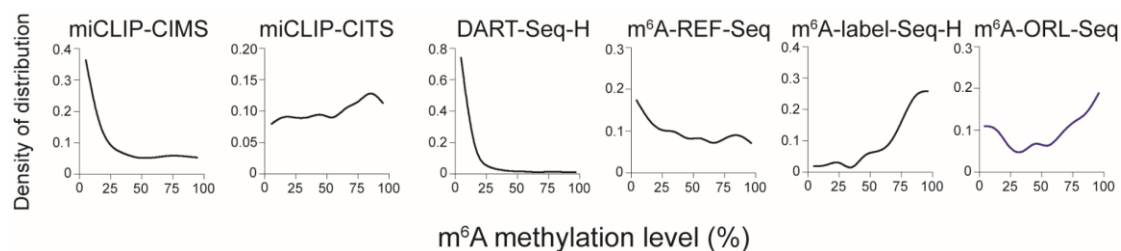

Fig. S24. Stoichiometry distribution of methylation levels of m^6A sites identified by different methods. Based on the dataset of MAZTER-Seq, methylation levels of m^6A sites identified by different methods can be analyzed. m^6A-ORL-Seq enables detect m^6A sites of low methylation levels.
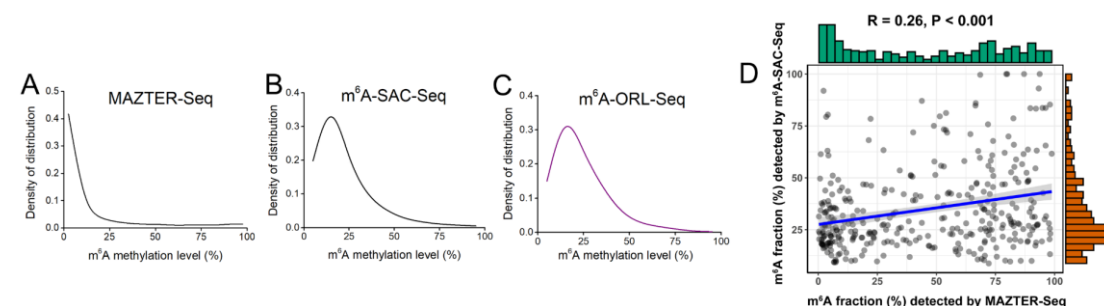

Fig. S25. (A) m^6A stoichiometry distribution revealed by MAZTER-Seq in HEK-293T transcriptome. (B) m^6A stoichiometry distribution revealed by m^6A-SAC-Seq in HEK-293T transcriptome. (C) Stoichiometry distribution of methylation levels of m^6A sites identified by m^6A-ORL-Seq based on the dataset of m^6A-SAC-Seq. (D) Correlation analysis between MAZTER-seq-based quantitations and m^6A-SAC-Seq-based quantitations.

18. Synthesis and data analysis of spike-in RNAs

The DNA template (117 nt) for spike-in RNAs (100 nt) were synthesized by Genecreate (Wuhan, China). The sequences are as followings. Underlined bases indicate the promoter of T7 RNA Polymerase. Sequences were provided as 5' to 3' order.

1) unmodified spike DNA (unmod-spike)
<u>TAATACGACTCACTATAGGG</u>TAGCGTTCATGCTAGTCATGCTAACTGTACATAGCGATCGATCTTTCAGA
GAAATTCGATTAAGGCAAATCGATCGATCAAGTAATGCGCTTCCTCT
unmodified spike DNA (complementary strand)
AGAGGAAGCGCATTACTTGATCGATCGATTTGCCTTAATCGAATTTCTCTGAAAGATCGATCGCTATGTA
CAGTTAGCATGACTAGCATGAACGCTACCCTATAGTGAGTCGTATTA

2) 10% m^{6}A spike DNA (each A was 10% modified with m^{6}A, 10%-spike)
<u>TAATACGACTCACTATAGGG</u>CCCCAATGGAAATAAGTCACCCCTTACGGAAACCCCAATGGAAATAAG
TCACCCCTTACGGAAACCCCAATGGAATAAAGTCACCCCTTACGGAAAC
10% m6A spike DNA (complementary strand)
GTTTCCGTAAGGGGTGACTTTATTCCATTGGGGTTTCCGTAAGGGGTGACTTATTTCCATTGGGGTTTCC
GTAAGGGGTGACTTATTTCCATTGGGGCCCTATAGTGAGTCGTATTA

3) single m^{6}A site spike-in (single-spike)
<u>TAATACGACTCACTATAGGG</u>TTTTTTGTGTCTTGCCTTTTTTCTTTTTTTTGGCTTTTTGCTTTCCTTCCC
T**A**TTCTGTTTGCCGCGTGCCTTCTTTTTCGGGTTTTCCTGTTTTCG
single m6A site spike-in (complementary strand)
CGAAAACAGGAAAACCCGAAAAAGAAGGCACGCGGCAAACAGAATAGGGAAGGAAAGCAAAAAGC
CAAAAAAAAGAAAAAAGGCAAGACACAAAAAACCCTATAGTGAGTCGTATTA

Spike-in RNAs were in-vitro transcribed by HiScribe T7 High Yield RNA Synthesis Kit (NEB) according to the manufacturer's protocol (NEB, RNA Synthesis with Modified Nucleotides, E2040). m^{6}ATP was purchased from TriLink.

1) unmod-spike RNA:
GGGUAGCGUUCAUGCUAGUCAUGCUAACUGUACAUAGCGAUCGAUCUUUCAGAGAAAUUCGAUU
AAGGCAAAUCGAUCGAUCAAGUAAUGCGCUUCCUCU
2) 10-spike RNA (each A was 10% modified with m^{6}A):
GGGCCCCAAUGGAAAUAAGUCACCCCUUACGGAAACCCCAAUGGAAAUAAGUCACCCCUUACGGA
AACCCCAAUGGAAUAAAGUCACCCCUUACGGAAAC
3) single-spike RNA:
GGGUUUUUUGUGUCUUGCCUUUUUUCUUUUUUUUGGCUUUUUGCUUUCCUUCCCU-m^{6}A-
UUCUGUUUGCCGCGUGCCUUCUUUUUCGGGUUUUCCUGUUUUCG

For each RNA sample, mixed with 0.01% each kind of spike-in RNAs. For example, 5.0 µg RNA was mixed with 0.50 ng unmod-spike RNA, 0.50 ng 10%-spike RNA, and 0.50 ng single-spike RNA. Each type of spike-in RNA was counted during the data analysis.
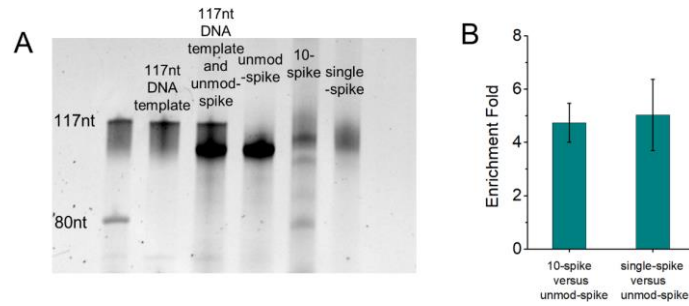

Fig. S26 (A) Denaturing PAGE confirmed the synthesis of spike-in RNAs, then RNA was purified by gel extraction. (B) Enrichment fold of m⁶A modified spike-in RNAs.
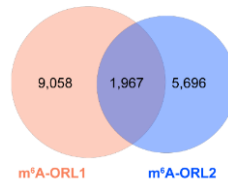
19. Overlapping extents between m⁶A-ORL samples

Fig. S27 Venn diagrams for the overlap between two m⁶A-ORL samples.

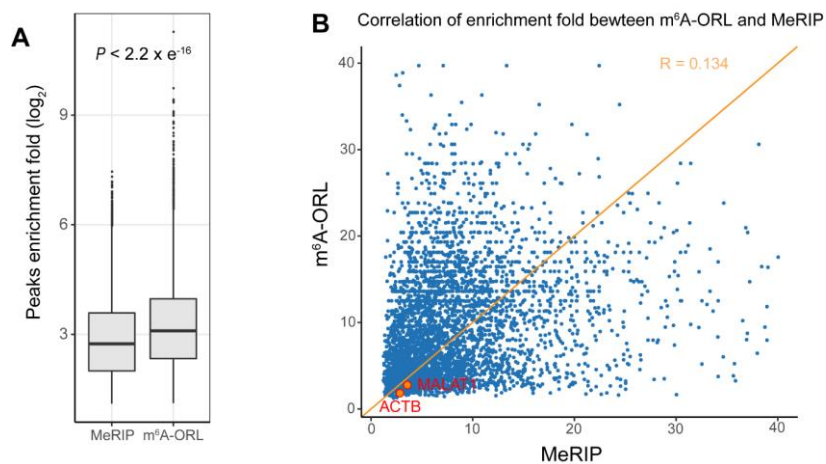## 20. Comparison for the enrichment fold between m⁶A-ORL and MeRIP

Fig. S28 (A) The overall enrichment fold of m⁶A-ORL peaks and MeRIP peaks. (B) The correlation of enrichment fold between m⁶A-ORL and MeRIP.

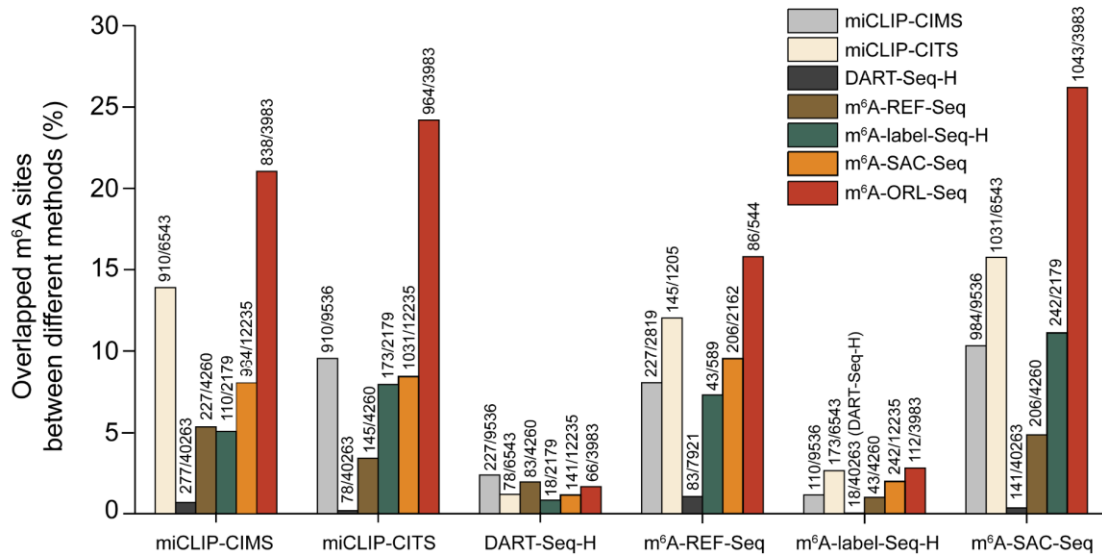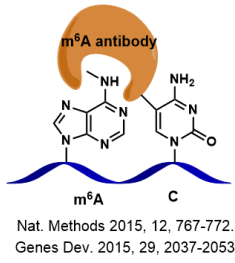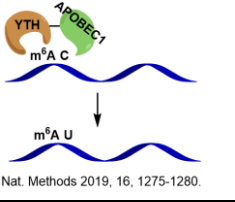## 21. Overlapping extents between the m⁶A datasets identified by different methods
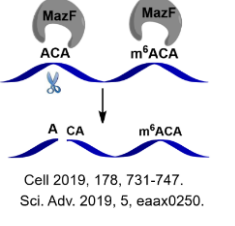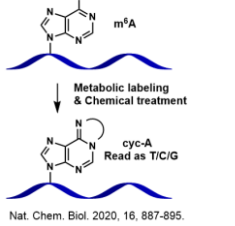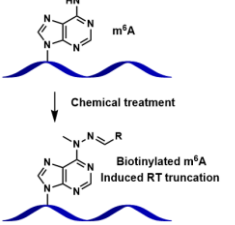

Fig. S29 Overlapping extents between the m⁶A datasets identified by different methods. H: High-confidence sites.

The m⁶A sites detected by m⁶A-ORL-Seq are the most reproducible.

22. Comparison of current base resolution methods for m⁶A profiling

Table S6. The strengths and limitations of the current base resolution methods for m^{6}A profiling.

	Schematic diagram	Principle	Strengths	Major concerns
miCLIP, m^{6}A-CLIP	 Nat. Methods 2015, 12, 767-772. Genes Dev. 2015, 29, 2037-2053.	m^{6}A antibody binding and UV-crosslinking between antibody and m^{6}A-containing RNA.	Most widely used for m^{6}A research at base resolution.	High input samples; abundant false-positive sites likely resulting from antibody cross-reactivity;[14] unable to quantify the methylation level.
DART-Seq	 Nat. Methods 2019, 16, 1275-1280.	Deamination of C adjacent to an m^{6}A.	Low input samples; enable the single-cell m^{6}A profiling[15] and estimation of m^{6}A level.	Abundant false positive caused by non-specific C-to-U editing.
MAZTER-Seq, m^{6}A-REF-Seq	 Cell 2019, 178, 731-747. Sci. Adv. 2019, 5, eaax0250.	MazF is an m^{6}A-sensitive endonuclease, that enables the cleavage of ACA motif.	Enable to quantify the methylation level.	Limited to m^{6}ACA sites; widespread false positives caused by the non-specificity of MazF.[16]
m^{6}A-label-Seq	 Nat. Chem. Biol. 2020, 16, 887-895.	Using artificial SAM for metabolic labeling, the m^{6}A sites were substituted by a^{6}A.	Enable the identification of clustered m^{6}A; could also be used for the detection of 6mdA in DNA.[17]	Using artificial SAM may affect the original methylation in cells and cause false m^{6}A sites.
m^{6}A-ORL-Seq		m^{6}A was selective converted into Bm^{6}A through three-step chemical labeling.	Most reproducible; not expensive; easy to scale up; could also be developed for the estimation of m^{6}A level and detection of 6mdA in DNA.	Deamination of A and C caused mutations in data analysis.

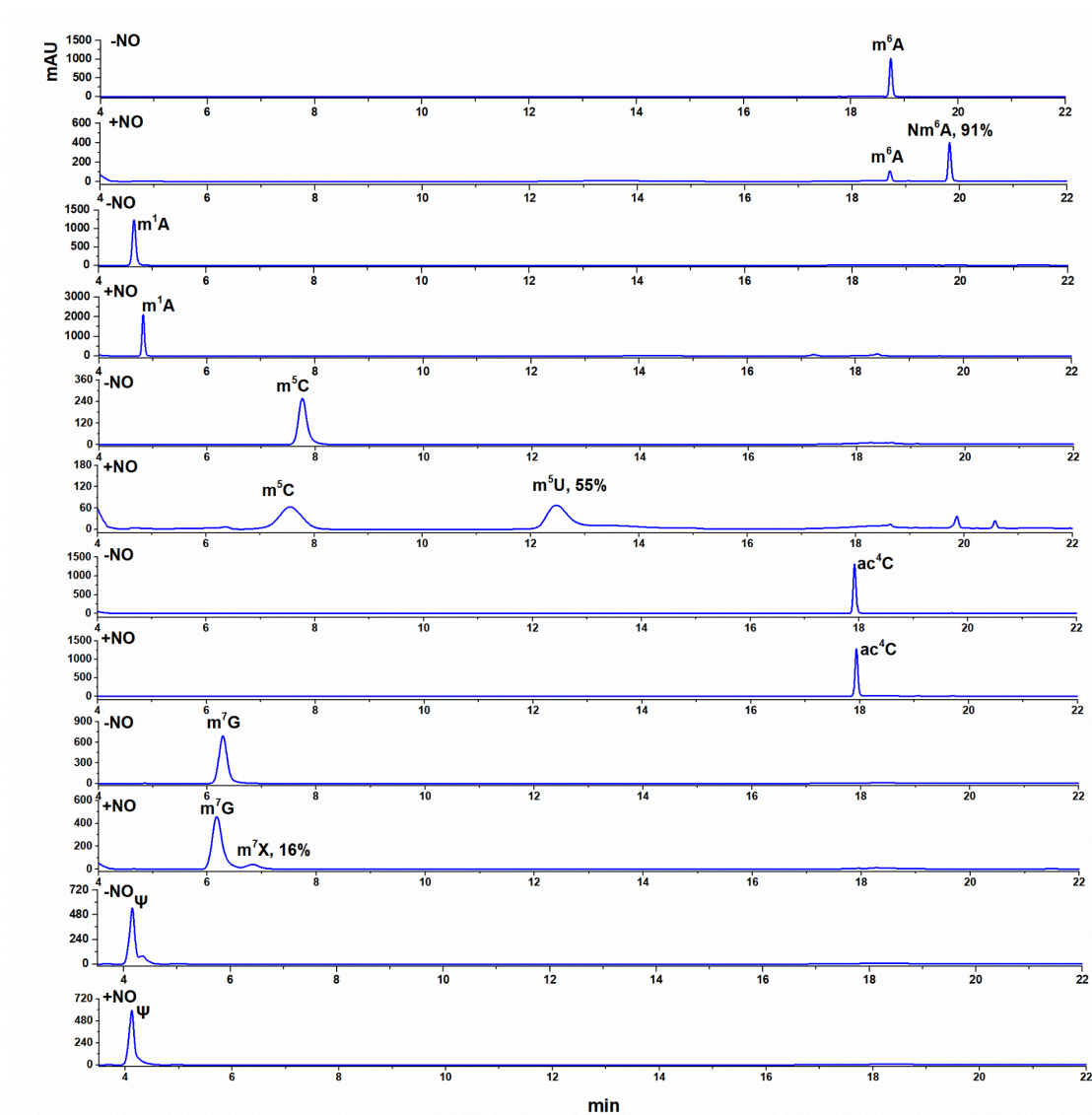## 23. NO bubbling for other abundant RNA modification

Fig. S30. HPLC monitored the conversion of modified nucleosides under NO treatment. Incubation conditions were the same as A/G/C/m6A nucleosides as stated on page S2. m^1A, ac^4C and Ψ did not react with NO/O_2, m^5C was converted into m^5U, and m^7G was converted into m^7X. Conversion rates were determined by HPLC quantification at 260 nm using external standards.
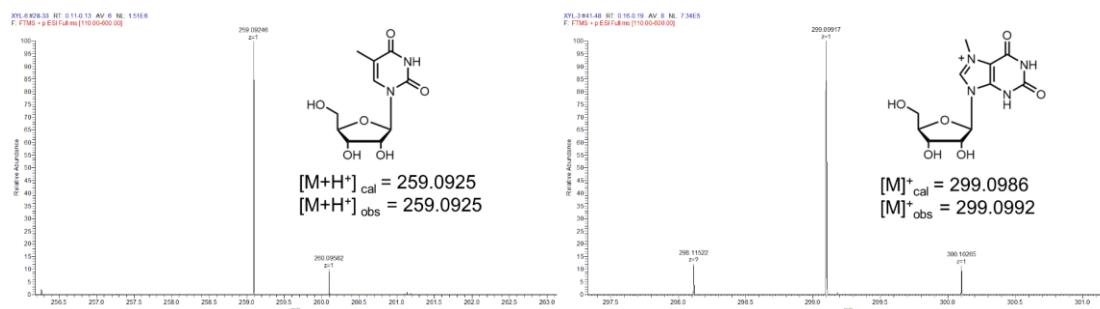

Fig. S31. HRMS confirmed the conversion of m^5C to m^5U and m^7G to m^7X.

24. References

[1]   M. Martin. Cutadapt Removes Adapter Sequences From High-Throughput Sequencing Reads. *EMBnet J.* **2011**, 17, 10-12.

[2]   A. Dobin, C. A. Davis, F. Schlesinger, J. Drenkow, C. Zaleski, S. Jha, P. Batut, M. Chaisson, T. R. Gingeras. STAR: ultrafast universal RNA-seq aligner. *Bioinformatics* **2013**, 29, 15-21.

[3]   A. O. Olarerin-George, S. R. Jaffrey. MetaPlotR: a Perl/R pipeline for plotting metagenes of nucleotide modifications and other transcriptomic sites. *Bioinformatics* **2017**, 33, 1563-1564.

[4]   Y. Xiao, Y. Wang, Q. Tang, L. Wei, X. Zhang, G. Jia, *Angew. Chem. Int. Ed.* **2018**, *57*, 15995-16000.

[5]   Y. Xie, Y. Wang, Z. He, W. Yang, B. Fu, G. Zou, X. Zhang, J. Huang, X. Zhou, *Anal. Chem.* **2020**, *92*, 12710-12715.

[6]   J. T. Bush, R. K. Leśniak, T.-L. Yeh, R. Belle, H. Kramer, A. Tumber, R. Chowdhury, E. Flashman, J. Mecinović, C. J. Schofield, *Chem. Commun.* **2019**, *55*, 1020-1023.

[7]   P. Chaudhary, S. Gupta, P. Sureshbabu, S. Sabiah, J. Kandasamy, *Green Chem.* **2016**, *18*, 6215-6221.

[8]   S. V. Makarov, A. K. Horváth, R. Silaghi-Dumitrescu, Q. Gao, *Chem. Eur.J.* **2014**, *20*, 14164-14176.

[9]   X. Li, X. Xiong, M. Zhang, K. Wang, Y. Chen, J. Zhou, Y. Mao, J. Lv, D. Yi, X.-W. Chen, C. Wang, S.-B. Qian, C. Yi, *Mol. Cell* **2017**, *68*, 993-1005.e1009.

[10]   H. Sun, K. Li, X. Zhang, J. e. Liu, M. Zhang, H. Meng, C. Yi, *Nat. Commun.* **2021**, *12*, 4778.

[11]   Y. Xie, Z. Fang, W. Yang, Z. He, K. Chen, P. Heng, B. Wang, X. Zhou, *Bioconjugate Chem.* **2022,** *33*, 353-362.

[12]   Y. Mahdavi-Amiri, K. Chung Kim Chung, R. Hili, *Chem. Sci.* **2021**, *12*, 606-612.

[13]   S. Werner, A. Galliot, F. Pichot, T. Kemmer, V. Marchand, M. V. Sednev, T. Lence, J.-Y. Roignant, J. König, C. Höbartner, Y. Motorin, A. Hildebrandt, M. Helm, *Nucleic Acids Res.* **2021**, *49*, e23.

[14]   S. Schwartz, Sudeep D. Agarwala, Maxwell R. Mumbach, M. Jovanovic, P. Mertins, A. Shishkin, Y. Tabach, Tarjei S. Mikkelsen, R. Satija, G. Ruvkun, Steven A. Carr, Eric S. Lander, Gerald R. Fink, A. Regev, *Cell* **2013**, 155, 1409-1421.

[15]   M. Tegowski, M. N. Flamand, K. D. Meyer, *Mol. Cell* **2022**. DOI: 10.1016/j.molcel.2021.12.038.

[16]   Z. Zhang, T. Chen, H.-X. Chen, Y.-Y. Xie, L.-Q. Chen, Y.-L. Zhao, B.-D. Liu, L. Jin, W. Zhang, C. Liu, D.-Z. Ma, G.-S. Chai, Y. Zhang, W.-S. Zhao, W. H. Ng, J. Chen, G. Jia, J. Yang, G.-Z. Luo, *Nat. Methods* **2021**, 18, 1213–1222.

[17]   M. Cheng, X. Shu, J. Cao, M. Gao, S. Xiang, F. Wang, Y. Wang, J. Liu, *ChemBioChem* **2021**, *22*, 1936-1939.